Energy Conversion and Management 297 (2023) 117745

Contents lists available at ScienceDirect

Energy Conversion and Management

journal homepage: www.elsevier.com/locate/enconman

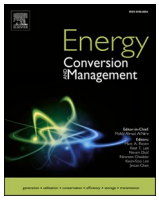

A comparative life cycle impact assessment for solar heat integration in post-combustion carbon capture

Kayla Kev [a,b], Nishant Modi [a,c], Dia Milani [a,*], Minh Tri Luu [b], Scott Nelson [b], Norhuda Abdul Manaf [d], Xiaolin Wang [c], Michael Negnevitsky [c], Ali Abbas [b]

[a] CSIRO Energy Centre, 10 Murray-Dwyer Circuit, Mayfield West, NSW 2304, Australia
[b] School of Chemical and Biomolecular Engineering, The University of Sydney, NSW 2006, Australia
[c] School of Engineering, University of Tasmania, Hobart, TAS 7005, Australia
[d] Department of Chemical and Environmental Engineering, Malaysia-Japan International Institute of Technology, Universiti Teknologi Malaysia, Kuala Lumpur, Malaysia

ARTICLE INFO

Keywords:
Post-combustion carbon capture
Solar-powered PCC
Solar collector field
Solvent storage
Solar multiple
Life cycle assessment

ABSTRACT

This study compares the life cycle assessment of conventional post-combustion carbon capture (PCC), solar-assisted PCC, and a novel concept of solar-powered PCC where the rich solvent is independently regenerated in the solar collector field at zero steam demand from the power-plant. Using the OpenLCA software and the EcoInvent database, the environmental impact of the proposed solar-powered PCC is compared with four main scenarios: power-plant only, power-plant with conventional PCC, optimised solar-assisted PCC at a 23 % solar fraction, and the ideal solar-assisted PCC at 100 % solar fraction. It is found that the levelized global warming potential per unit of electricity production for the solar-powered PCC is the lowest among all scenarios (865 $kg_{CO2\text{-}eq}$/MWh). Therefore, the CO_2 abatement relative to the base-case scenario is the highest (191 $kg_{CO2\text{-}eq}$/MWh), resulting in a global warming reduction of 18.1 % for the 660MW_e and 38.1 % for the 330MW_e power-plants, respectively. Moreover, the global warming abatement in the solar-powered PCC scenario proportionally increases with the solar multiple, as the solvent storage requirements are proportionally reduced. However, increasing the solar multiple value does not render the process more economically feasible. Despite the absence of an energy penalty for the power-plant with solar-powered PCC scenario, this advantage alone is not sufficient to offset the economic challenges associated with the large solar collector field and solvent storage installation. Overall, efforts to reduce the cost of CO_2 capture using solar-powered PCC will be greatly advantageous for retrofitting this novel technology into existing coal-fired power-plants or industrial plants to mitigate global warming.

1. Introduction

The reduction of global warming is the world's persistent priority and is becoming increasingly urgent. As a representative greenhouse gas (GHG) and one of the primary contributors to climate change, CO_2 emissions in 2021 increased by approximately 4.2 % to bounce back to the unprecedented levels of 36.7 gigatonne recorded in 2019 before the Covid-19 pandemic [1]. This is directly attributed to the ongoing consumption of fossil fuels in power generation, transport, and other industrial activities, where coal accounts for approximately 37 % of the global electricity generation by fuel [2]. To avoid the consequences of exacerbated climate change, carbon capture and storage (CCS) technologies are necessary to achieve the goals of the Paris Agreement in 2015 [3]. There is a broad scientific consensus that not only GHG emissions need to be significantly limited, but also a wide range of negative emissions technologies would be necessary to reach the net

Abbreviations: CC, Carbon credit; CCS, Carbon capture and sequestration; CFC, Chlorofluorocarbons; CFD, Computational fluid dynamics; DAC, Direct air capture; GHG, Greenhouse gas; GWP, Global warming potential; HTF, Heat transfer fluid; HX, Heat exchanger; LCA, Life cycle analysis; LCI, Life cycle inventory; MEA, Monoethanolamine; NZE, Net-zero emissions; PCC, Post-combustion carbon capture; PP, Power plant; PTC, Parabolic trough collector; REC, Renewable energy certification; SA-PCC, Solar-assisted PCC; SCF, Solar collector field; SF, Solar fraction; SM, Solar multiple; SP-PCC, Solar-powered PCC; So-St, Solar stripper; TES, Thermal energy storage.

* Corresponding author.
E-mail address: dia.milani@csiro.au (D. Milani).

https://doi.org/10.1016/j.enconman.2023.117745
Received 10 May 2023; Received in revised form 2 October 2023; Accepted 5 October 2023
Available online 12 October 2023

zero emissions (NZE) goals [4]. This can be achieved by decarbonising energy-intensive industrial activities, where the global transition towards NZE by 2050 can be realized by leveraging effective CCS technologies. According to the Intergovernmental Panel on Climate Change [5], a shortage of CCS technologies in the next few decades would cause an increase of 29–297 % in total mitigation costs when compared to default technology assumptions (scenarios without CCS but with other low-carbon technologies) which indicates that further studies on CCS technologies are critical.

Post-combustion carbon capture (PCC) is one of the most promising and accessible CCS technologies for commercial applications [6]. In particular, absorption-based PCC would require minimal retrofitting and does not demand costly adjustments to existing power-plants (PP)s [7]. However, the key challenge for the wide adoption of the PCC is the high thermal energy penalty it incurs, which accounts for 19.5–40 % of the total PP capacity [8], and the consequences on revenue reduction. This can be partially offset by integrating solar thermal technology with the PCC system [9]. One strategy to accomplish this is via solar-assisted PCC (SA-PCC), where part of the necessary steam for solvent regeneration is sustained from the solar collector field (SCF). The SCF provides a partial supply of thermal energy that reduces the steam bled from the main power cycle and helps to increase the PP capacity [10]. Fig. 1 illustrates the concept of SA-PCC where a heat exchange network is established to dynamically respond to the reboiler thermal energy demand where possible. A tow-tank thermal energy storage (TES) system is used to mitigate the transient conditions. Solar thermal input into PCC-retrofitted power-plants, also called 'solar repowering', can be implemented by either the injection or recirculation methods. The first is via the installation of an individual boiler to deliver the required steam for the solvent regeneration process and avoid steam extraction from the power-plant steam cycle. The second method is to extract equivalent regeneration energy from the PP steam cycle, but use an adequately-sized SCF to compensate for the lost electricity and prevent capacity reduction [11]. Cau et al. [12] conducted a comparative performance analysis of different integrating approaches, based on the design of the SCF to produce low-pressure saturated steam for the PCC solvent regeneration process and intermediate-pressure saturated and superheated steam for the introduction in the steam cycle. Both options would require a large investment in SCF and an exorbitant cost for thermal energy storage (TES) to maintain nonstop operation when solar energy is unavailable.

More recently, solar-powered PCC (SP-PCC) was also proposed to eliminate the energy penalty from the PP such that the process would fully be reliant on solar energy [13]. In this process, the CO_2-rich solvent leaving the absorber was directly pumped to the SCF to run across the receiver tubes of solar collectors [14]. The SCF consists of a network of solar-stripper (So-St) modules positioned parallel to each other, allowing the rich solvent to directly absorb the solar thermal energy and release CO_2 gas in the process [15]. The geometry design of the So-St unit was analysed and optimized using a computational fluid dynamics (CFD) platform to address the internal thermo-physical complications associated with the multicomponent boiling flow where the

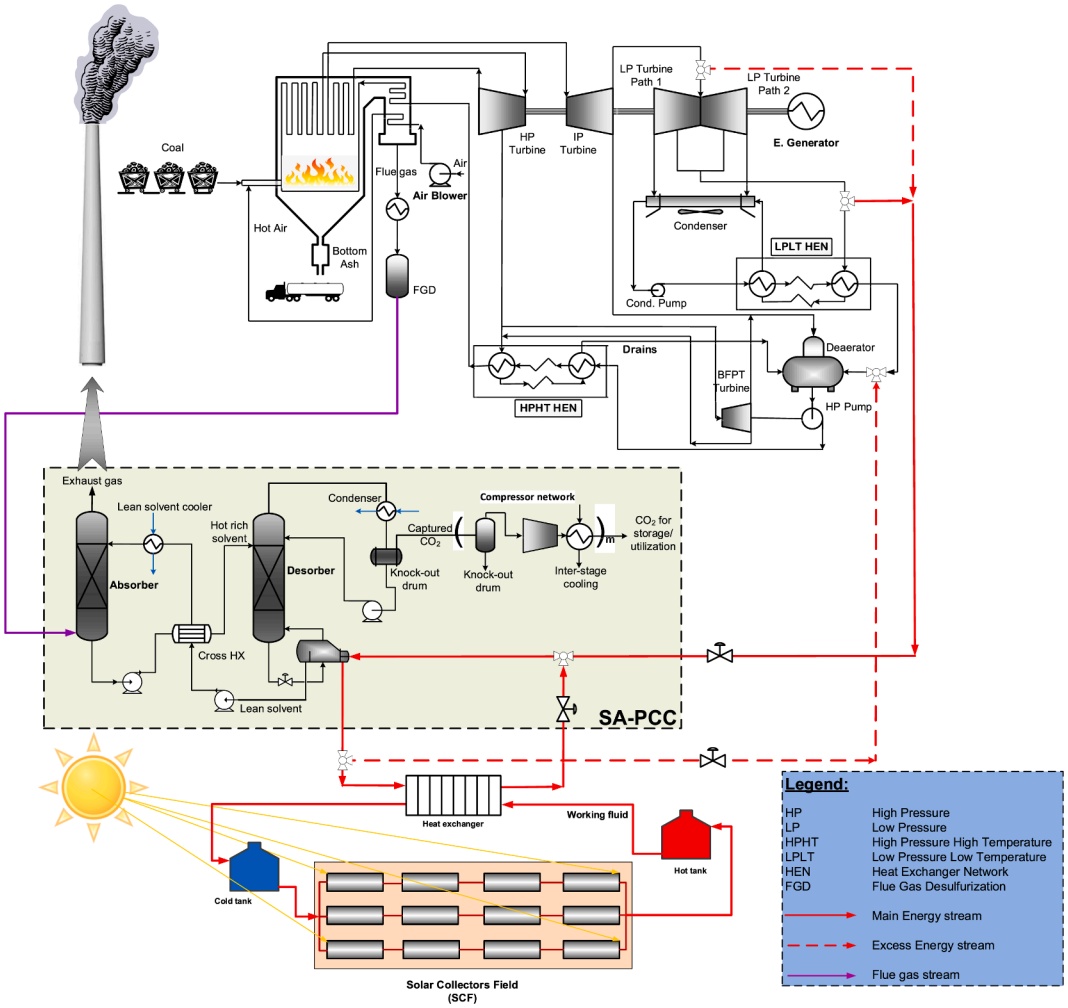

Fig. 1. A schematic of a coal-fired power-plant with PCC sourcing the reboiler duty by integrating the solar thermal energy into the power-plant steam cycle (SA-PCC).

reaction kinetics would change with the thermodynamics under transient conditions [16]. The key challenge of this superstructure is in synchronizing the steady-state operation of the absorber, with the dynamic operation in So-St network, which would require advanced process control strategies to ensure that the So-St network can operate transiently while achieving the CO_2 capture target throughout seasonal variation of the year [17]. Since the desorption process occurs directly in the SCF, this configuration would eliminate the conventional desorption unit of the PCC, consisting of the stripper and reboiler. Hence, there would be a significant trade-off in the cost of the desorption unit with the added SCF and solvent storage, which was fully addressed in comparative detailed techno-economic studies [18]. However, the full-scale environmental burdens of the SP-PCC relative to the typical PCC and SA-PCC counterparts remain unclear. Hence to solarise PCC operation and utilise renewable energy away from the PP steam cycle, the concept of SA-PCC is elevated to a new frontier of SP-PCC as illustrated in Fig. 2. Consequently, it is expected that the global warming potential (GWP) of the latter would be better-off because the generated steam in the PP is utterly used for power generation only, while the CO_2 content in the flue gas is largely captured via the SP-PCC.

It is widely acknowledged that any new technology being proposed must not impose a significant burden on the environment. This can be assessed using life cycle analysis (LCA), a method of systematic analysis of the environmental impacts associated with products or services during their entire life. The LCA is a well-established assessment tool to determine environmental hotspots for various CCS strategies, with wide recognition among academic and industrial practitioners [19]. It is an effective approach to holistically model the environmental impact of a product system throughout its lifecycle [20]. Although, LCA has been standardised in ISO 14040/14044 [21], the methodological choices and scopes have not been strictly defined. There is no common framework clearly available for estimations and benchmarking [22]. As a result, LCA studies on various CCS technologies have not been often comparable [23].

Numerous studies have been conducted on LCA for PCC plants, when compared to other available CCS methods. Zhang et al. [24] found that the monoethanolamine (MEA) based PCC scenario had higher environmental stress due to solvent degradation and emissions compared to gas separation via membrane processes. Alternatively, the hybrid process showed even lower environmental impact as a result of less fossil fuel-based power consumption. Due to the wider scope of this research, the focus was on the interrelationship of the energy analysis and negative consequences on the environment rather than the LCA itself, which must be taken into account. Contradictory to this, Matin and Flanagan's study [25] found that the MEA-based carbon capture system presented better performance compared to the ammonia-based unit in terms of the carbon and water footprints. They also reported that the addition of a CO_2 capture unit was only advantageous in terms of GWP, where other environmental categories such as fossil fuel depletion, ionizing radiation and marine eutrophication, exhibited higher impacts than the baseline scenario (i.e. without a carbon capture unit). Similar observations were made by Petrescu et al. [26] while evaluating a pulverised coal-fired PP coupled with and without PCC. The results align with Matin and Flanagan's study [25] as the PCC effectively lowers the GWP, but other environmental impact factors might be worsened. In this context, the literature indicates that CCS technologies are efficient means to decrease

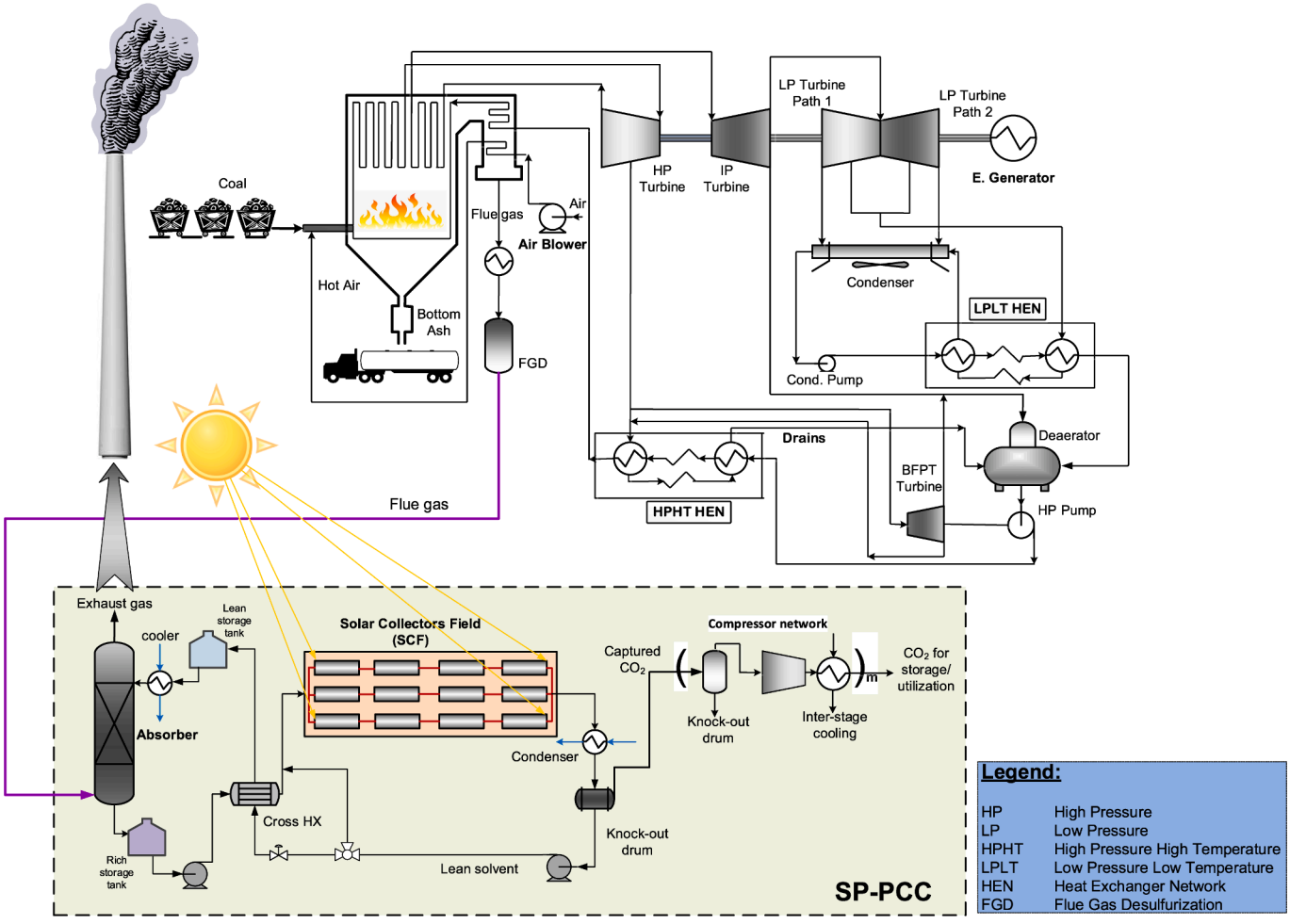

Fig. 2. Schematic of SP-PCC retrofitted to a PP where the SCF comprises the So-St network is replacing the typical desorption unit of the PCC.

the consequences of GWP and climate change. There is, however, a trade-off that must be considered with other environmental issues, where the LCA should be conducted for various PCC systems including those integrated with solar thermal energy as a measure to mitigate fossil fuel-based energy consumption.

Literature reveals that limited studies have been conducted on LCA for the solar integrated PCC. Wang et al. [27] analysed SA-PCC processes through an LCA approach, integrating both life cycle GHG assessment and cost, with reference to a coal-fired PP in China. It highlighted that the solar-assisted repowering process for CCS has substantial benefits in mitigating GHGs and the total cost. This study [27] was able to cross-examine the results from both methodologies to understand the potential of SA-PCC technologies. However, it focused on each of the life cycle stages independently and was unable to account for other important elements that may pose negative environmental impacts. In Manuilova et al.'s [28] work, the environmental performance of a CO_2 capture project in Saskatchewan (Canada) was evaluated using an LCA method as defined by the ISO 14000 standards. The TRACI life cycle impact assessment tool was used to convert life cycle inventory data into environmental effects [28]. The results proved that there was a reduction in the GWP and air impact factors when comparing a coal-fired PP with and without PCC. Since this was a cradle-to-grave study with an emphasis on the electric power generating station, it lacks a detailed assessment of the other stages of the lifecycle such as post-production and end-of-life. Similar to Wang et al.'s research [27], potential environmental consequences, such as ionising radiation and photochemical oxidant formation, was excluded due to the limited scope of the study.

Recent LCA studies have exceeded the traditional fossil fuel-based energy systems to assess technologies labelled as negative emission technologies, namely bioenergy with CCS (BECSS) and direct air capture (DAC). For example, Carpentieri et al. [29] studied the LCA of an integrated biomass gasification combined cycle as a mean of carbon–neutral energy source and assessed the reduction in both GHG emissions and natural resource depletion. Weihs et al. [30] and Xie et al. [31] investigated the effects of biomass co-firing with carbon capture and storage using LCA. Several studies have been conducted on the LCA of DAC systems which extracts CO_2 directly from the atmosphere. De Jonge et al. [32] assessed the life cycle carbon removal efficiency of a DAC system at high temperatures and quantitatively scored the main environmental factors. Since this study only focused on the life cycle carbon efficiency, it failed to include other potentially important elements that would adversely impact the environment. Moreover, Deutz and Bardow [4] conducted a full LCA for the Climework's DAC plants in Hinwil (Switzerland) and Hellisheidi (Iceland) and found that it achieved GHG removal efficiencies of 85 % and 93 %, respectively. The results highlighted that the climate benefits of DAC strongly depend on the energy source, aligning with the conclusions made by De Jonge et al [32]. As such, these additional aspects must be considered into the system framework of a comprehensive LCA to evaluate the environmental impacts and trade-offs of CCS technologies. Moreover, the energy demand for solvent regeneration in conventional PCC is typically supplied by bleeding steam from the existing steam cycle in the PP. This steam is often generated via coal combustion and is typically expanded in steam turbines to generate electricity [33]. Bleeding part of the steam for the purpose of solvent regeneration in the PCC would require burning more coal to generate more steam for the same capacity of the PP. Numerous studies have been conducted on the economic impacts of partial steam bleeding in the PCC process. For instance, Li et al. [34] investigated the technical and economic performance of the MEA-based PCC process integrated with a 650-MW coal-fired PP, Tsupari et al. [35] studied the same for steel mill, and Dave et al. [36] examined the liquid absorption based PCC processes for both existing and new pulverised coal-fired power stations in Australia. However, there is limited research on the consequences that may lead to further environmental degradation, resource depletion, or human health implications [37]. The limited research on LCA for the PCC [38] and SA-PCC counterparts [39] has relatively analysed the main contributors of environmental burdens. To the best of the authors' knowledge, there are no studies that assessed the environmental consequences for the SP-PCC as an emerging CCS technology. As a result, more work needs to be done to address the LCA impact assessment for the SP-PCC relative to other carbon capture options with clearly defined system boundaries.

This paper, therefore, evaluates the environmental footprint of the SP-PCC system in comparison to the conventional PCC and SA-PCC counterparts across all stages of the life cycle. It aims to identify, classify, and quantify the environmental hotspots through a comprehensive cradle-to-grave LCA assessment. First, the life cycle inventories for all technology blocks are collected starting from coal production, the PP, the PCC, and all the way to CO_2 compression, dehydration, and transport to the sequestration site. Then, the midpoint impact categories are analysed using the prominent ReCiPe method within the OpenLCA (v.1.10) software and the results are compared across five distinct scenarios. Following this, a sensitivity analysis for the level I impact category, namely the climate change, is conducted to recognize the main block contributors to the GWP across all five scenarios. Finally, the GWP impacts of the two largest parameters (SCF vs solvent storage) in the SP-PCC category are also compared to evaluate their GWP influence on the levelized cost of electricity at different solar field sizes. This work is very critical to understand the LCA implications for process hybridization with renewables, where in this case is aiming to ultimately achieve an independent and modularized solar-powered carbon capture.

2. Modelling approach

The modelling approach starts by defining the goal and scope of this comparison, then comparing different system boundaries, gathering the life cycle inventories for major block components, to finally conduct the impact assessment for different scenarios. The main goal of this LCA is to quantitatively determine the absolute environmental burdens of each scenario and examine whether the proposed SP-PCC configuration can add major environmental benefits in reference to other carbon capture scenarios.

2.1. System boundaries

The first step in conducting a resourceful LCA comparison is defining representative system boundaries based on the material journey starting from raw materials extraction to the end of its life [23]. Some system boundaries such as gate-to-gate only focus on the internal processes within the manufacturing plant boundaries, only covering the factory limits from the entry gate to the exit gate [40]. The selection of resources, product use and disposal phase are not included in this assessment, which limits the scope of the LCA. Cradle-to-gate assessment overcomes this hurdle and assesses the product lifespan impact from resource extraction to the end of the manufacturing stage. However, it excludes the application and use of the product itself, making it effective when it is infeasible to cover the entire lifecycle including reuse, recycling, or final disposal [41]. To address this shortcoming, a cradle-to-grave scope was introduced to take this assessment further through the product use until disposal at the end-of-life stage to calculate and compare different impact categories. This is desirable for studies that aim to assess the environmental burdens across the product lifecycle from the extraction of raw materials to the disposal or landfill phase [26]. Nowadays, more progressive cradle-to-cradle scopes are defined to create a full ecological loop assessment where the product materials are eventually decomposed and recycled to become an input to the initial cradle [42]. This paradigm is orientated towards eco-effectiveness and a circular economy, which has only been introduced more recently. The design principles of a cradle-to-cradle approach stem from a zero-waste perspective, concentrating on continuous innovation and improvement [43]. However, achieving a closed cycle of material exchange with complete waste recovery typically requires significant social and

infrastructure changes that are not easily incorporated into existing systems. As a result, a LCA via cradle-to-cradle is an emerging assessment tool with design strategies that must be refined to provide solutions that are sustainable in the long term [43].

In this LCA study, a comparative cradle-to-grave method is conducted on the emerging SP-PCC relative to the conventional PCC and SA-PCC counterparts to assess their environmental impact and potential to reduce GHG emissions. This covers the initial extraction and transport of coal, processing and firing the coal to produce electric power, capturing the CO_2 from the flue gas, and all the way to the CO_2 compression and transportation to the sequestration stage. This approach further takes the waste disposal and decommissioning methods at the end of the project life into consideration. Fig. 3 provides a visual representation of the LCA boundaries for a PCC process. A gate-to-gate assessment for this process illustrated by the LCA boundaries box often focus more on the chain of events inside the boundary (dash-lined rectangle), leaving the elements external to the box uncovered, which is limiting the breadth of the study. Therefore, the cradle-to-grave LCA system boundary method is chosen as it has a greater breadth compared with the gate-to-gate and cradle-to-gate methods. It also has a great validity when compared to the cradle-to-cradle framework, since there is no clear path linking the CO_2 product removed from the process to the initial coal extraction or even a valid utilization pathway that keeps the CO_2 in the loop.

2.2. Scenario comparison

In this study, the SP-PCC configuration is compared with four other scenarios as shown in Fig. 4. Scenario (A) represents the reference case of a standalone PP without connection to a CO_2 capture unit; scenario (B) represents a PP integrated with a conventional PCC; scenario (C) for a PP integrated with a SA-PCC where the size of the SCF is optimised for the best potential revenue; scenario (D) for a PP integrated with a SA-PCC where the SCF equipped with adequate thermal energy storage (TES) is sized to independently provide all thermal energy demand in the PCC and no steam is extracted from the PP; and finally scenario (E) represents the SP-PCC where the solvent is directly regenerated in the SCF. Detailed descriptions of each scenario can be found in the earlier technoeconomic study [18].

The difference between scenarios (C) and (D) around the solar field sizing and the percentage of solar contribution in the nominal load to offset the energy penalty from the power-plant. The percentage of SCF contribution in the SA-PCC scenario would merely depends on economic justifications and the government incentive programs that can support this scenario. Fig. 5 displays the effect of SF variation on the PP with SA-PCC case at different potential government incentive programs for the Sydney case-study. Four SA-PCC incentive programs were sensitized and compared from 0 to 100 % SF. The first case represents the basic case-study with no value for captured CO_2 and no government support scheme (Fig. 5- the black solid line). The second case represents a government subsidy proportional to the SF (SCF size). It is assumed that a maximum of $2M subsidy is provided to any SF less than 10 % of the plant capacity (Fig. 5- the red dot-dash line). Above 10 % SF, this subsidy increases proportionally to the SF increase and is capped at $30 M when SF reaches 70 % of the plant capacity. Any SF above the 70 % cap would still be entitled to the maximum cap of $30 M. The third case represents the carbon credit (CC) revenue gained from carbon tax (Fig. 5- the green dot line) where the four simulations presented in Fig. 5 are categorized based on carbon price schemes. The fourth case represents a combined revenue from the subsidy scheme and renewable energy certificate (REC) scheme estimated at $35/MWh generated either directly from renewable energy sources or above a certain baseline as a result of renewable energy implementation (Fig. 5- the blue dashed line). For the base case at low carbon prices (e.g. $11.53/tonne$_{CO2}$) [6], the PP operator would not generate any positive revenue from the implementation of SA-PCC even at large SF values. When the carbon price is almost doubled to $23/tonne$_{CO2}$, however, the fourth case related to 'subsidy + REC' program starts to capture little positive revenue around 23 % SF (Fig. 5- red dot). This revenue would be largely visible when carbon price $\geq$$44/tonne$_{CO2}$ for the third and fourth cases as evident by the red and yellow dots. It is clear that an SF of ~23 % shows the highest potential revenue for the third and fourth cases only of SA-PCC in the Sydney case-study, and therefore this SF of 23 % is selected as the economically optimised solar contribution value for a representative SA-PCC scenario. Additionally, the SF of 100 % scenario is also chosen for SA-PCC as it represents an idealistic process that operates at the same level as SP-PCC to become a completely independent process from the power-plant steam cycle. Similar to the techno-economic study [18], having two SA-PCC scenarios for comparison, rather than the 23 % SF alone, allows a fair assessment of the LCA for SA-PCC and SP-PCC systems as it compares the environmental effects to be examined under similar assumptions (e.g. 100 % SF). The following subsections explain the life cycle inventories and impact assessment method used in this LCA study.

2.3. Life cycle inventory and assumptions

The life cycle inventory (LCI) phase gathers and quantifies energy and material inputs, waste outputs and emissions data for a specific process across the system boundary. It models the product system according to the LCA scope, revealing the interactions between the system

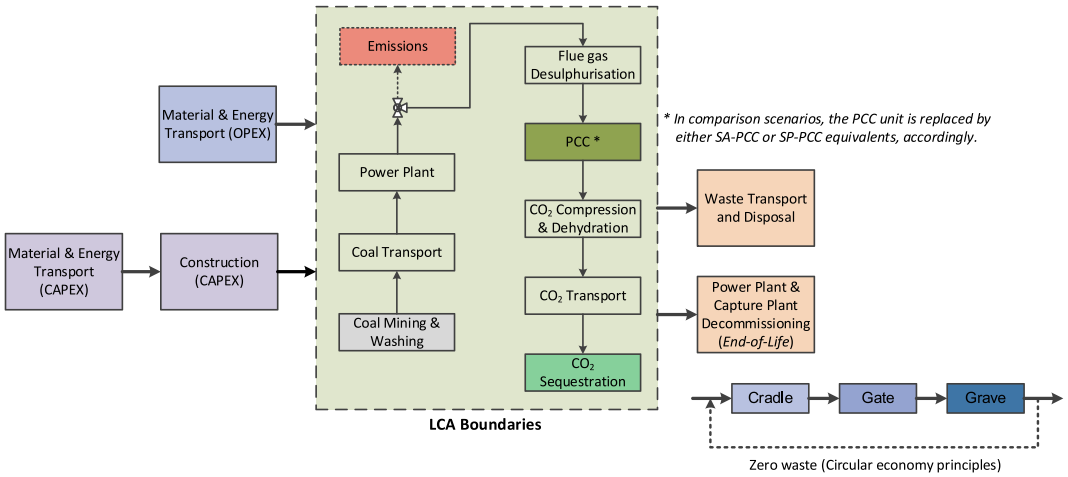

Fig. 3. The LCA appraisal block diagram. The cradle-to-grave framework is selected in this comparison to account for the environmental impact from the basic raw material extraction up to the end-of-life stage.

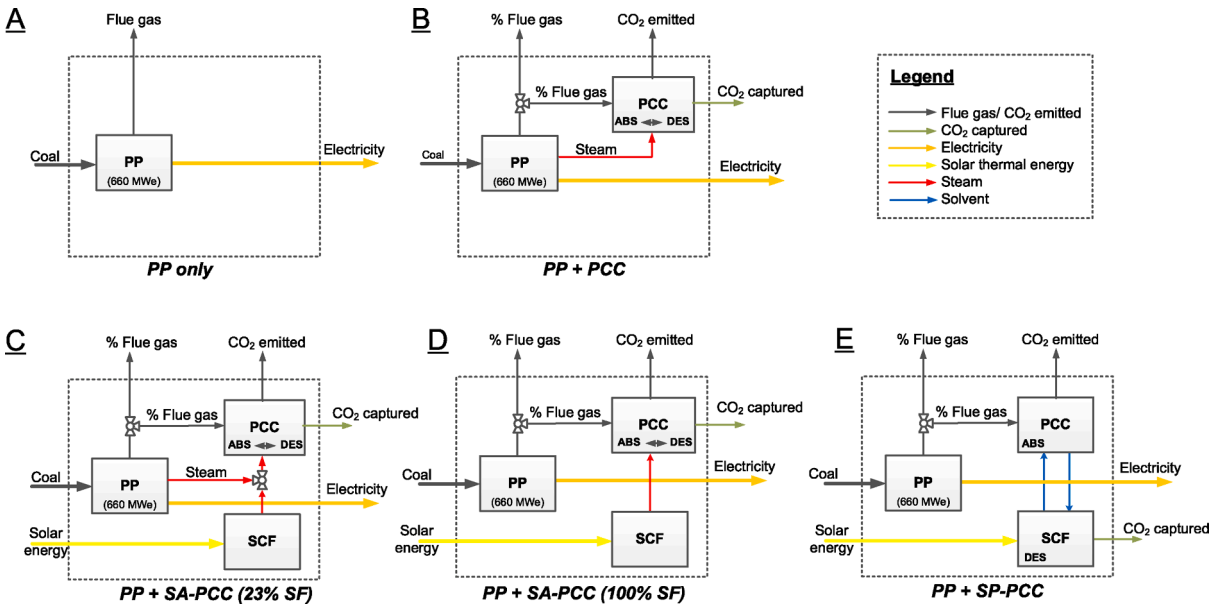

Fig. 4. Block diagram of five scenarios set for LCA comparison. Scenario (A) a PP-only; (B) for a PP integrated with a typical PCC; (C) for a PP integrated with a solar-assisted PCC at an optimal 23 % SF; (D) for a PP integrated with a solar-assisted PCC at the idealistic 100 % SF; and (E) is for a PP integrated with a solar-powered PCC.

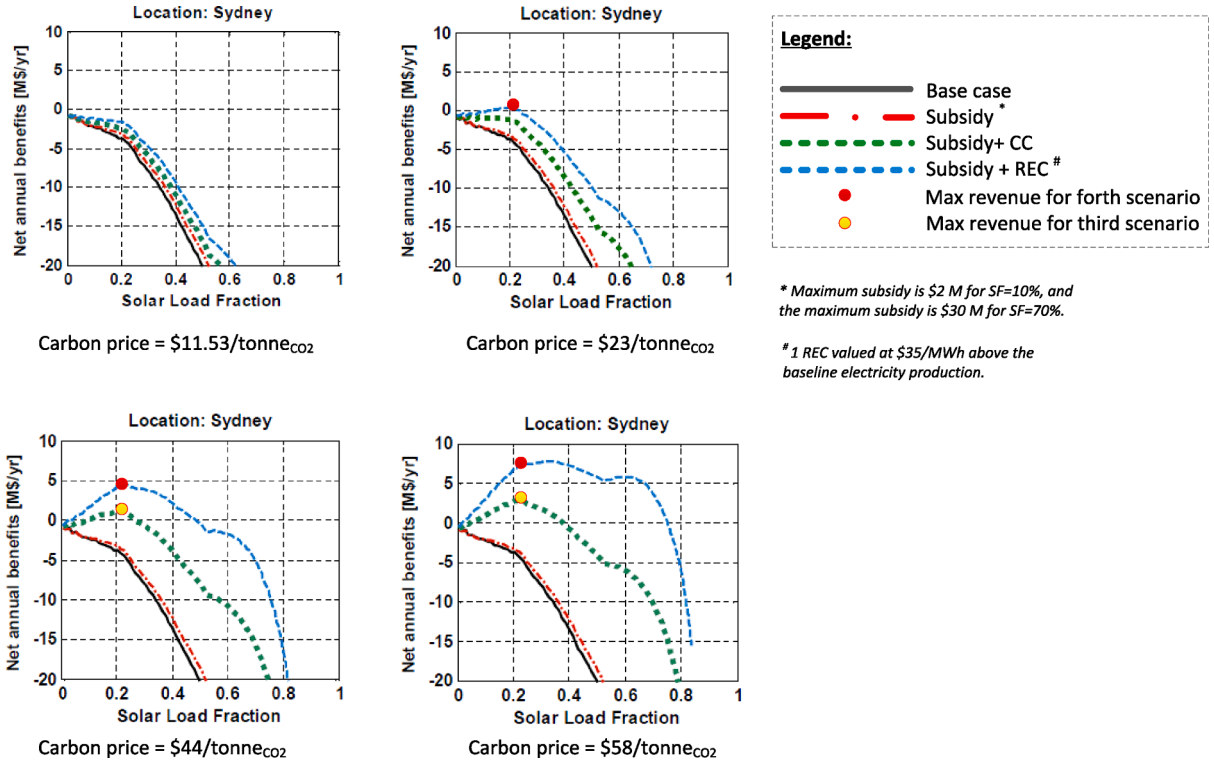

Fig. 5. The net annual profit trends for the power-plant owners/operators when combined with SA-PCC at different government incentive programs and for various carbon price schemes.

inputs and outputs [23]. In this work, the LCI data are collected from the Aspen® model design. The Aspen® model design was validated against the experimental data and the validation method has been published in the Supplementary Materials of the earlier work [14]. The So-St design parameters were computed for Sydney case-study are summarized in Table 1. These design parameters were later refined and optimised in a comprehensive design protocol applicable anywhere in the world [15].

The assumptions used are similar to the work of Fimbres Weihs et al. [44]. All energy and material values that span across the whole project lifetime are levelized to capture one unit (1 tonne) of CO_2. This is because all capital energy and mass flows are initial inputs with impacts that must be distributed over the project lifespan. Therefore, a capital multiplier is calculated and used as the scaling factor to account for this, as shown in Eq. (1) [44]. It also assumes that there is no social discount factor for future CO_2 emissions. The following subsections present the general requirements when choosing inventory sets and modelling

Table 1
The finalized So-St field design for Sydney case-study [17].

	Design variables	Design value
Specification for one So-St module	Rich loading at So-St module entrance	0.45
	Lean loading at So-St module exit	0.22–0.21
	All-liquid velocity in 1st segment (m/s)	1.2
	Segments per a So-St module	6
	Solvent flowrate in one module (kg/hr)	18,119
	Design vapor molar fraction (VMF)	0.05
	Energy demand (MJ/kg_{CO2})	10.2
Overall So-St field design	Total solvent from absorber (kg/hr)	2,378,710
	Number of solvent loops	22
	Number of So-St arrays	22
	Number of So-St modules per array	6
	Total So-St length per module (m)	109.9
Length of So-St segment in one module	Segment 1 (m)	23.6
	Segment 2 (m)	20
	Segment 3 (m)	18.1
	Segment 4 (m)	16.9
	Segment 5 (m)	16.0
	Segment 6 (m)	15.3
	Total (m)	109.9
Overall So-St field design	Total solvent from absorber (kg/hr)	2,378,710
	Number of solvent loops	22
	Number of So-St arrays	22
	Number of So-St modules per array	6
Parabolic trough design	Nominal solar heat flux (kW/m)	1
	Aperture width (m)	7
	Absorber (tube) inner diameter (m)	0.076
	Absorber (tube) outer diameter (m)	0.08
	Glass envelop inner diameter (m)	0.115
	Glass envelop outer diameter (m)	0.12

frameworks to bridge data gaps.

$$Capital\ Multiplier = \frac{CO_2\ functional\ unit}{CO_2\ over\ lifespan} = \frac{1\ t_{CO2}}{1.5 \times 10^6\ \frac{t_{CO2}}{y} \times 30\ y} = 2.22 \times 10^{-8} \quad (1)$$

2.3.1. Coal production

Coal production consists of mining and washing to prepare the coal for use in PPs. Bituminous (black) coal is assumed as the base fuel for use in power generation, and the *EcoInvent 3.6* database is used as the inventory that calculates coal properties and environmental impacts. This considers the emissions from inputs and outputs of the coal mining operation and preparation stages. For the transport of coal, the PP location is assumed to be within 30 km of the mine site: 20 km by rail and 10 km by conveyor. This arrangement is generally adopted at the NSW power plants of Mt. Piper, Bayswater and Eraring [44]. The required electrical energy is assumed to be supplied from the Australian power grid.

2.3.2. Power plant (PP)

All inputs and outputs need to be considered for the PP inventory, and Table 2 summaries the inventory assumptions. It is assumed that 34 % of the flue gas from the power-plant is processed in the PCC unit, and that this processed flue gas has a 90 % CO_2 capture efficiency to eventually capture 1.5 megatonne of CO_2 per year [45]. Values for specific CO_2 emissions and coal calorific value are assumed, and the coal input flow is then levelized to the 1 tonne CO_2 capture unit [44]. The water consumption requirements are based on published values [46]. Fly ash emissions from the PP and construction requirements are based on data from the National Renewable Energy Lab [47]. The main construction materials assessed are concrete, steel, aluminium and iron, and all minor materials such as plastics, copper, wood and glass are assumed negligible due to inadequate data. The LCI for construction accounts for the emissions of the construction material production processes. This analysis excludes the emissions produced during the construction process because of incomplete data, and this is considered less significant when compared with other factors as it is a capital input. During the decommissioning phase of the PP, it is assumed that 75 % of materials used in the construction can be recovered and reused as scrap metal in secondary metal production operations, while the remaining percentage is sent to a landfill [47].

As a result of the differences in SF contribution, the energy output from the PP changes in all scenarios, with the most notable variation being observed in SA-PCC, as outlined in Table 3. For the desorber unit, the energy requirements are constant across the PCC and SA-PCC scenarios, where the thermal energy output from the PP steam creates an additional energy penalty related to the overall electricity generation. Additionally, Table 3 reveals that the desorption energy demand for SP-PCC is larger than the other scenarios since the regeneration of CO_2-rich MEA solvent within the So-St configuration causes a larger thermal energy requirement. Although the calculated energy penalties are lower than the reported energy penalties in the range of 19.5–40 % as reported in Parvareh et al. [10], this is because only 34 % of the flue gas from the reference 660MW_e PP is being processed rather than the whole amount. If all the flue gas was processed at a CO_2 capture rate of 90 %, then the energy penalty would nearly triple and fall within the literature range.

Table 4 presents the composition of the flue gas, where the Aspen® model was used to determine the mass flowrate and composition of the flue gas. The Aspen® model only contains the major components of the flue gas stream, in particular H_2O, CO_2, O_2 and N_2, while SO_2, NO_x and

Table 2
Summary of the PP inventory assumptions.

Factor	Value	Units	Reference
CO_2 captured	1	tonne	–
CO_2 capture efficiency	90	%	–
Processed flue gas in the PP	34	%	[45,48]
Specific CO_2 emissions	0.874	tonne/MWh	[44]
Coal calorific value	23.8	MJ/kg coal	[44]
Higher heating value efficiency	36	%	[44]
Electrical energy generated	3.74	MWh_e	Aspen®
Thermal energy generated	10.386	MWh_t	Aspen®
Total coal input	1.571	tonne	–
Boiling and cooling water	146.3	L/MWh_e	[46]
Emissions and waste			
CO_2 captured	1	tonne	–
CO_2 processed by PCC (34 %)	1.11	tonne	–
CO_2 unprocessed (66 %)	2.16	tonne	–
CO_2 total PP emissions	3.27	tonne	–
Fly ash specific emissions	26,580	kg/GWh_e	[47]
Fly ash emissions	99.4	$kg/tonne_{CO2}$	–
Coal transport			
Freight distance	20	km	–
Conveyor distance	10	km	–
Construction			
Concrete	158,758	kg/MW_e	[47]
Steel	50,721	kg/MW_e	[47]
Aluminium	419	kg/MW_e	[47]
Iron	619	kg/MW_e	[47]
Construction materials recovery	75	%	[47]

Table 3
Power Plant Energy Outputs Across Four Scenarios.

Parameter	PCC	SA-PCC (23 %)	SA-PCC (100 %)	SP-PCC	Units
Solar fraction	0	23	100	100	%
Desorber energy requirements					
Total	1.04	1.04	1.04	2.44	$MWh_t/tonne_{CO2}$
	3.74	3.74	3.74	8.78	$GJ_t/tonne_{CO2}$
Solar contribution	0	0.24	1.04	2.44	$MWh_t/tonne_{CO2}$
	0	0.86	3.74	8.78	$GJ_t/tonne_{CO2}$
PP steam contribution	1.04	0.80	0	0	$MWh_t/tonne_{CO2}$
	3.74	2.88	0	0	$GJ_t/tonne_{CO2}$
PP energy outputs					
Net thermal energy	9.34	9.59	10.39	10.39	$MWh_t/tonne_{CO2}$
	33.62	34.52	37.40	37.40	$GJ_t/tonne_{CO2}$
Net electrical energy	3.36	3.45	3.74	3.74	$MWh_t/tonne_{CO2}$
	12.10	12.42	13.46	13.46	$GJ_t/tonne_{CO2}$
Energy penalty on the PP	10	7.7	0	0	%

Table 4
Summary of flue gas composition.

Parameter	Value	Units	Reference
Main flue gas components (per tonne of CO_2 in the flue gas)			
H_2O	0.187	$tonne/tonne_{CO2}$	Aspen®
O_2	0.336	$tonne/tonne_{CO2}$	Aspen®
N_2	3.878	$tonne/tonne_{CO2}$	Aspen®
SO_2	0.0019	$tonne/tonne_{CO2}$	[44]
NO_x	0.0022	$tonne/tonne_{CO2}$	[44]
Trace flue gas components (per tonne of CO_2 in the flue gas)			
Si	0.018501	$kg/tonne_{CO2}$	[44]
Fe	0.003307	$kg/tonne_{CO2}$	[44]
Mg	0.000824	$kg/tonne_{CO2}$	[44]
Ti	0.000389	$kg/tonne_{CO2}$	[44]
Ca	0.000321	$kg/tonne_{CO2}$	[44]
K	0.000183	$kg/tonne_{CO2}$	[44]
Ba	0.000114	$kg/tonne_{CO2}$	[44]
Mn	0.000057	$kg/tonne_{CO2}$	[44]
P	0.000034	$kg/tonne_{CO2}$	[44]
V	0.000023	$kg/tonne_{CO2}$	[44]

trace elements are neglected to ensure computational simplicity. As a result, the emissions data for the excluded components were obtained from Fimbres Weihs et al. [44], and these emissions were considered for the unprocessed flue gas in the PP. It is assumed that the processed flue gas is cleaned of these components through the electrostatic precipitator, desulfurization and the de-NO_X units.

2.3.3. PCC

Key differences arise from the PCC inventory for different capture scenarios, and the chemical emissions of these are tabulated in Table 5. The main emissions including CO_2, MEA and water were based on the Aspen® Model. Minimal emissions in gaseous, aqueous and solid forms were accounted for based on literature values [38]. These emissions were assumed to be constant across all scenarios, since they primarily emerge from the absorber unit which is kept a constant parameter.

The capacities of the lean cooling heat exchanger for the absorber and the condenser for the desorber are constant, enabling a calculation of the equivalent cooling water mass based on the specific heat formula (Eq. (2). The water temperature gradient is based on an assumed 10 °C pinch.

$$Q_C = m_w C_{p,w} \Delta T \tag{2}$$

where Q_c is the total cooling duty, m_w is the cooling water mass flowrate, $C_{p,w}$ is the specific heat capacity of water, and ΔT is the water temperature difference based on an assumed 10 °C pinch. To calculate vessel masses, the following equation (Eq. (3) is used:

$$V = \frac{\pi H((D+2t)^2 - D^2)}{4} + 2\frac{\pi t(D+2t)^2}{4} \tag{3}$$

where V is the cylindrical surface volume, D is the vessel diameter, H is the vessel height and t is the vessel thickness. The first term in Eq. (3) calculates the mass of the cylindrical vessel and the second term accounts for the top and bottom ends of the vessel. A summary of the variables used across the four scenarios is presented in Table 6. Based on the Aspen® model, the impact of MEA and water inputs are determined on capital and operational flows, where the SP-PCC process requires more MEA and water because of the extensive solvent storage. The electrical power demand for the flue gas blower and rich solvent pump remains constant across all scenarios. However, the electrical output of the cycle pump varies to pump the solvent across the SCF due to its large size. A 5 % auxiliary factor was assumed to account for any extra

Table 5
Assumptions for PCC Chemical Emissions.

Parameter	Value	Units	Reference
Emission to air			
CO_2	111	$kg/tonne_{CO2}$	Aspen®
Monoethanolamine	42.7	$g/tonne_{CO2}$	Aspen®
Ammonia	1.8	$g/tonne_{CO2}$	[38]
Formaldehyde	4.3	$g/tonne_{CO2}$	[38]
Acetaldehyde	4.7	$g/tonne_{CO2}$	[38]
Acetone	5.2	$g/tonne_{CO2}$	[38]
Methyl amine	3.4	$g/tonne_{CO2}$	[38]
Acetamide	0.0011	$g/tonne_{CO2}$	[38]
Emission to water			
Monoethanolamine	2.14	$kg/tonne_{CO2}$	Aspen®
Water	667.8	$kg/tonne_{CO2}$	Aspen®
Ammonia	0.4	$g/tonne_{CO2}$	[38]
Diethanolamine	0.0044	$g/tonne_{CO2}$	[38]
Formaldehyde	0.0001	$g/tonne_{CO2}$	[38]
Acetone	0.0023	$g/tonne_{CO2}$	[38]
Methyl amine	0.0012	$g/tonne_{CO2}$	[38]
Solid			
Gypsum	4.3	$kg/tonne_{CO2}$	[38]

Table 6
PCC components and assumptions.

Parameter	Value	Units	Reference
Heat exchangers (HX)			
Condenser duty	0.532	$MWh/tonne_{CO2}$	Aspen®
Lean cooling HX duty	0.502	$MWh/tonne_{CO2}$	Aspen®
Total cooling duty	1.035	$MWh/tonne_{CO2}$	Aspen®
Water specific heat capacity	4.18	kJ/kg K	–
Water temperature gradient (70–25 °C)	45	K	–
Cooling water mass	19.8	$tonne/tonne_{CO2}$	–
Solvent PCC construction			
Vessel thickness	14.7	mm	[49]
Steel density	7850	kg/m^3	[44]
Construction materials recovery	75	%	[47]
PTC construction			
Galvanised steel	0.98	kg/MWh	[50]
Stainless steel	0.029	kg/MWh	[50]
Low iron float glass	0.65	kg/MWh	[50]
Ceramic	0.0033	kg/MWh	[50]
Silicone	0.0033	kg/MWh	[50]
Borosilicate glass	0.043	kg/MWh	[50]
Concrete	0.00032	m^3/MWh	[50]
Construction materials recovery	75	%	[47]

equipment not considered in the standard PCC process. Furthermore, the breakdown of the vessel construction material requirements and solar parabolic trough collector (PTC) construction materials are also shown in Table 6. The materials for the PTC construction are determined based on the energy capacity required for the SCF.

2.3.4. Compression, dehydration, transport and sequestration

Table 7 summarises the inventory for compression, dehydration, transport and sequestration of the CO_2 product. The CO_2 compression stage is imperative for allowing the ease of CO_2 transport within the pipeline, and the specifications are based on literature data [48]. The work required for compression was calculated as follows (Eq. (4)):

$$W = \frac{ZRT}{M} \times \frac{N\gamma}{\gamma - 1}\left[\left(\frac{P_2}{P_1}\right)^{\frac{\gamma-1}{N\gamma}} - 1\right] \quad (4)$$

Where Z is the compressibility; R is the ideal gas constant (J/mol K); T is the suction temperature (K); M is the gas molar mass (g/mol); N is the number of compressor stages; γ is the heat capacity ratio; P_1 is the inlet pressure; and P_2 is the outlet pressure. The electricity for compression is calculated according to Eq. (5).

Table 7
Inventory for compressor, pipeline transport and sequestration.

Factor	Value	Units	Reference
Compressor			
Compressibility	0.9942	–	[44]
Ideal gas constant	8.3145	J/mol K	–
Suction temperature	303.15	K	[48]
Molar mass	44.01	g/mol	–
Inlet pressure	2	bar	Aspen®
Outlet pressure	110	bar	[48]
Heat capacity ratio	1.2938	–	–
Compressor stages	4	–	[48]
Isentropic efficiency	0.8	–	[44]
Mechanical efficiency	0.99	–	[44]
Work	256.2	MJ/tonne$_{CO2}$	–
Electricity	89.9	kWh/ tonne$_{CO2}$	–
Pipeline construction			
Pipeline distance	850	km	[44]
Pipeline diameter	0.3	m	[44]
Pipeline thickness	8.53	mm	[44]
Steel density	7850	kg/m^3	[44]
Pipeline mass	55,168,000	kg	–
Insulation (Rockwool) area	1,602,212	m^2	–
Pipeline recompression			
Specific pressure loss	0.06	bar/km	[52]
Specific booster stations	1	/100 km	[53]
Number of booster stations	9	–	–
Pressure loss per booster station	5.67	bar	–
Work per booster station	0.75	MJ/tonne$_{CO2}$	–
Electricity per booster station	0.26	kWh/ tonne$_{CO2}$	–
Total recompression electricity	2.38	kWh/ tonne$_{CO2}$	–
Pipeline emissions			
Fugitive CO_2 emissions	2.32	tonne$_{CO2}$/ (km y)	[52]
Sequestration			
Construction and decommissioning emissions	0.12	kg$_{CO2}$/ tonne$_{CO2}$	[51]
Electricity consumption	7	kWh/ tonne$_{CO2}$	[51]
Scaling factor	2	–	Scale 1.5 to 3 km
Scaled emissions	0.24	kg$_{CO2}$/ tonne$_{CO2}$	[51]
Scaled electricity consumption	14	kWh/ tonne$_{CO2}$	[51]
Construction materials recovery	75	%	[47]

$$E = \frac{W}{\eta_{is}\eta_m} \quad (5)$$

where η_{is} is the isentropic efficiency and η_m is the mechanical efficiency of the compressors. The assumptions for the transportation stage are based on Fimbres Weihs et al. [44], which gathered pipeline specifications based on an integrated carbon capture and storage economic model. The sequestration site is in Darling Basin, with a total transport distance of 850 km, as shown in Fig. 6. The sequestration inventory is based on Yujia et al. study [51] which assumes six injection wells with depths of 1.5 km over a 30-year lifespan. Their study [51] derived values for the indirect CO_2 emissions of construction and decommissioning, as well as the specific electrical consumption of the sequestration site.

2.4. Impact assessment

In this study, the ReCiPe Midpoint method is utilised to quantify the results of the LCI into a set of impact indicator scores [54]. ReCiPe is a life cycle impact assessment (LCIA) method that translates emissions and resource extractions into a specific number of environmental impact scores by means of so-called characterisation factors. The accumulation of these characterization factors would transitionally create damage pathways (midpoint) that eventually may cause irreversible damage to one or more of three endpoint categories namely, damage to human health, damage to ecosystem, and/or damage to the resource availability. A detailed description of the ReCiPe method is provided in the Supplementary Materials and the impact categories assessed are summarized in Table 8. The scenarios were modelled using OpenLCA (v.1.10) software, with the *EcoInvent 3.6* database integrated as a source of the emissions data for the life cycle boundary.

3. Results and discussions

This section explains the results obtained from the LCA for these five different scenarios. First, the midpoint environmental impacts of a 660MW$_e$ capacity PP are discussed. Then, the discussion focuses on the level I impact categories, namely ozone depletion and climate change as classified by Fazio et al. [55]. Finally, the results from the sensitivity analysis of the climate change category are discussed to further justify the importance of the proposed system. Fig. 7 illustrates the environmental trade-offs for these five scenarios on 13 impact factors for the same amount of coal intake. The following five factors are excluded as they exhibit zero impact across all scenarios: metal depletion, agricultural land occupation, natural land transformation, urban land occupation, and fossil depletion. The impact results provided by OpenLCA, are measured in 'emissions per tonne of CO_2 captured', which allows a direct comparison of various PCC units since they capture the same amount of CO_2. These values are then levelized to become unitless on a scale of zero to one, by taking a ratio of the direct emissions to the absolute maximum of any particular impact category across all five scenarios.

Compared to power-plant only (Fig. 7-a), the typical PCC scenario presented in Fig. 7-b reduces the shaded region of almost all impact categories except toxicities, ionising radiation, and ozone depletion, amplifying the potential environmental benefits of utilizing the PCC for capturing CO_2 emissions. A marginal increase in toxicities, ionising radiation and ozone depletion is likely attributed to the impact of MEA depletion in the PCC unit.

In comparing the conventional PCC with the 23 % SA-PCC system, it is found that integrating solar energy at 23 % SF marginally reduces the particular matter formation, terrestrial ecotoxicity and terrestrial acidification impacts (averagely by 4.37 %). This might be attributed to the reduction of associated atmospheric emissions (SO_x, NO_x, etc.) as a result of the reduced energy penalty in the SA-PCC unit. Contradictory to this, it increases the human toxicity and freshwater eutrophication

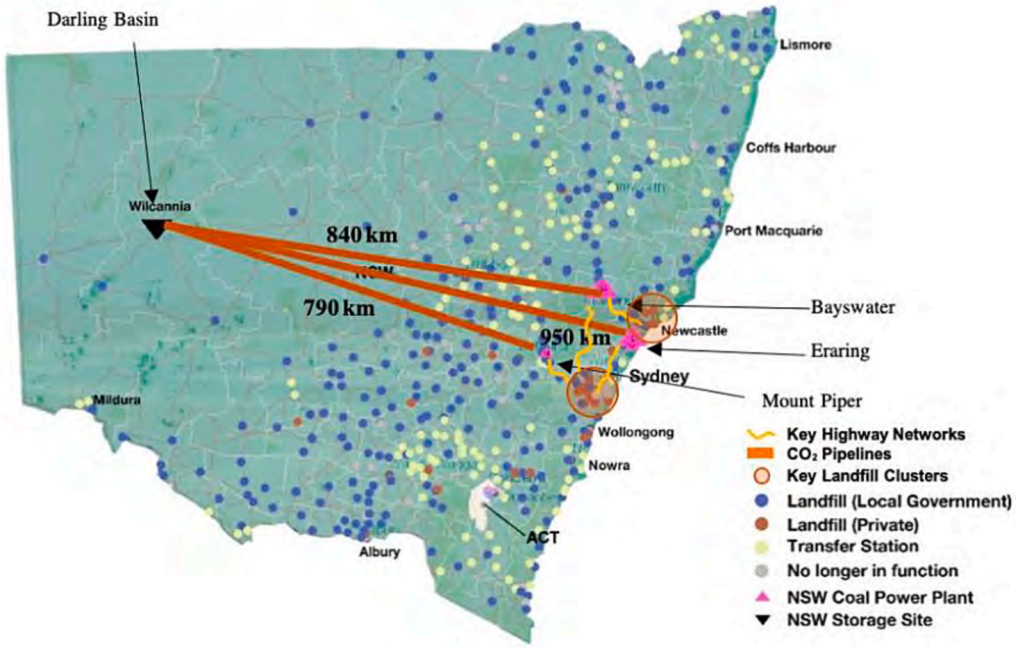

Fig. 6. Map of the pipeline transport distances from three power-plants (Mt. Piper, Bayswater and Eraring) to the Darling Basin sequestration site as calculated by Fimbres Weihs et al. [44].

Table 8
Impact categories for the ReCiPe Midpoint method considered in this study.

Impact Category	Units
Water depletion (WDP)	m^3
Terrestrial acidification (TAP100)	$kg_{SO2\text{-}eq}$
Ionising radiation (IRP_HE)	$kg_{U235\text{-}eq}$
Climate change (GWP100)	$kg_{CO2\text{-}eq}$
Photochemical oxidant formation (POFP)	kg_{NMVOC}
Human toxicity (HTPinf)	$kg_{1,4\text{-}DCB\text{-}eq}$
Metal depletion (MDP)	$kg_{Fe\text{-}eq}$
Ozone depletion (ODPinf)	$kg_{CFC\text{-}11\text{-}eq}$
Agricultural land occupation (ALOP)	m^2a
Marine ecotoxicity (METPinf)	$kg_{1,4\text{-}DCB\text{-}eq}$
Terrestrial ecotoxicity (TETPinf)	$kg_{1,4\text{-}DCB\text{-}eq}$
Marine eutrophication (MEP)	$kg_{N\text{-}eq}$
Natural land transformation (NLTP)	m^2
Freshwater ecotoxicity (FETPinf)	$kg_{1,4\text{-}DCB\text{-}eq}$
Freshwater eutrophication (FEP)	$kg_{P\text{-}eq}$
Particulate matter formation (PMFP)	$kg_{PM10\text{-}eq}$
Urban land occupation (ULOP)	m^2a
Fossil depletion (FDP)	$kg_{oil\text{-}eq}$

impacts by 7.20 % and 8.20 %, respectively due to the increased emissions of Manganese, Arsenic, Phosphate, etc. in waterways. It is important to note that the ozone layer depletion and climate change impacts remain almost the same in both scenarios. However, integrating solar energy is advantageous because it increases the capacity of power generation.

As shown in Fig. 7-d and 7-e, the 100 % solar-driven PCC systems via SA-PCC and SP-PCC concepts are advantageous for the climate change impact category only as the shaded region of all other categories has increased substantially. The environmental benefits of a 100 % SA-PCC system significantly deteriorate across all impact categories (Fig. 7-d) mostly attributed to the massive solar field environmental impacts at both manufacturing and also end-of-life disposals. The use of massive thermal energy storage (TES) would also have extensive construction and heat transfer fluid (HTF) nitrate salt requirements, in addition to the implications related to the change of land-use. This analysis proves that substantially increasing the SF ratio to increase renewable energy penetration might also have underlying environmental impacts that could exceed the short-term economic benefits. Therefore, an unbiased assessment must take all techno-economic and life cycle categories into account.

Relative to the 100 % SA-PCC scenario, the SP-PCC configuration lowers all major impact categories except human toxicity, marine ecotoxicity, marine eutrophication, freshwater eutrophication and freshwater ecotoxicity. The reductions are measured as 4.22 % in climate change impact and 46.2 % in ozone layer depletion. The main reason for this significant reduction is related to the elimination of HTF nitrate salts-based TES which has contributed by 62.8 % to the ozone depletion in the case of a 100 % SA-PCC scenario. This justifies the benefits of employing SP-PCC over 100 % SA-PCC without compromising the overall power output from the PP. In comparing Fig. 7-c and 7-e, the 23 % SA-PCC remarkably demonstrates less environmental impact than the SP-PCC, however, the PP would still have to bear a significant energy penalty. Therefore, the SP-PCC configuration may present a reasonable compromise for industrial emissions, particularly for industries that do not have steam production in their normal operation, where the establishment of a reliable heat source would have significant underpinning environmental impacts.

3.1. level-I category assessment

Among those 13 categories, two categories have more interest in literature and their impact often classified in level-I category, namely the ozone depletion and the climate change. Ozone depletion refers to the decrease in the density of the ozone layer which results in ultraviolet radiation reaching the Earth's surface, primarily caused by chlorofluorocarbons (CFCs) [56]. Notably, the potential for ozone depletion remains relatively consistent in all scenarios, except for SA-PCC 100 % where it significantly increases to its maximum value as illustrated in Fig. 7-d. This increased likelihood is mainly attributed to the addition of multiple processes and equipment involved in the operation of the PCC unit at 100 % SF [57]. This includes a massive TES system which requires an extensive construction of thermally insulated storage tanks, piping network, and bulky nitrate-salt HTF which brings a notable environmental impact and hence results in a greater ozone layer depletion rate. This further proves that increasing the solar penetration

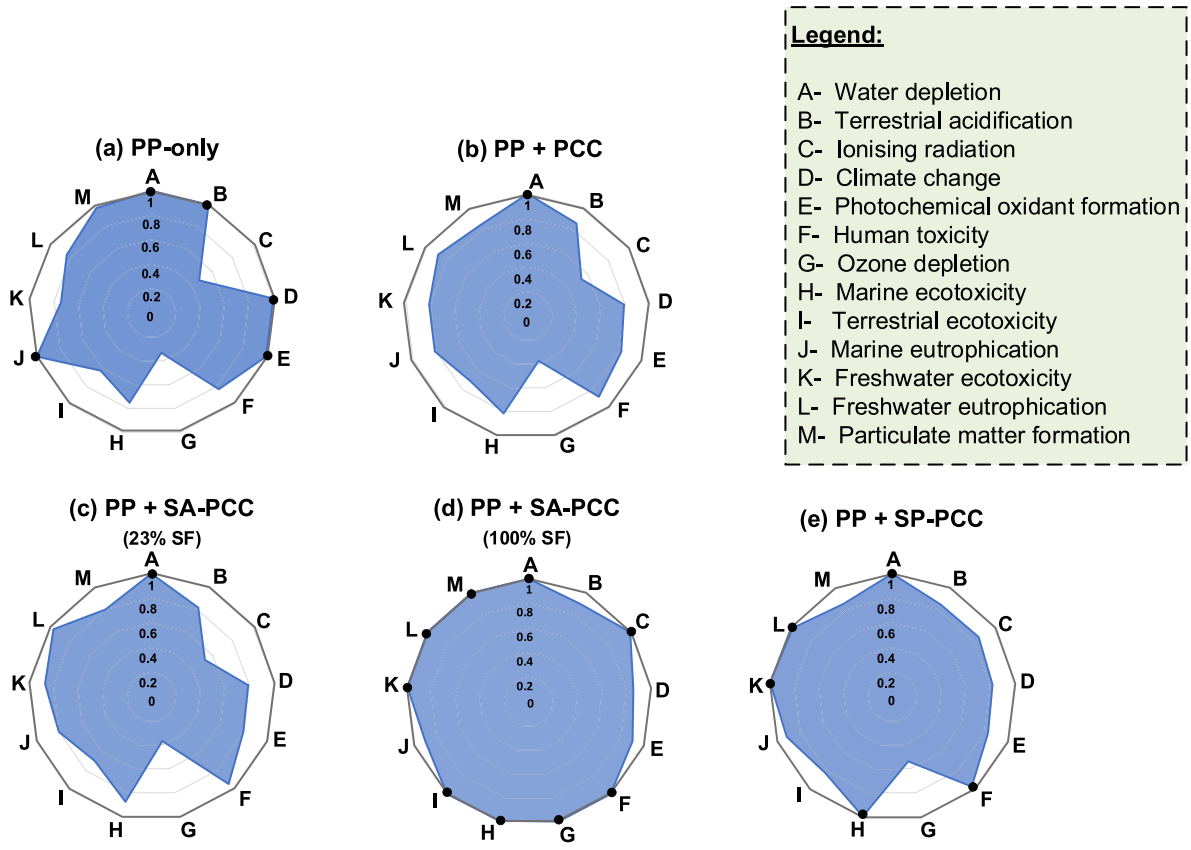

Fig. 7. Spider charts illustrating thirteen impact categories for 660MW$_e$ PP across five scenarios.

in the SA-PCC unit, by increasing the SF ratio, such that the heat duty of the reboiler is independent from the PP steam cycle might not be a fully environmentally benign process. Unlike SA-PCC, the SP-PCC configuration does not have this drawback as it can attain lower GHG emissions without relying on the PP steam cycle.

The climate change, the second level-I category quantified by the GWP index, allows comparisons of the amount of energy the emissions of 1 ton of a gas absorbed over a given period, usually a 100-year averaging time, compared with the emissions of 1 ton of CO_2 [58]. Fig. 8-a shows a comparison of the GWP impact for all five scenarios for the same amount of coal input into the system, with impacts levelized as 'emissions per tonne of CO_2 captured'. Furthermore, the results are also converted to 'emissions per MWh' power production which are presented in Fig. 8-b. As outlined in Fig. 8-b, the GWP for PP-only is 1,056 $kg_{CO2\text{-}eq}$/MWh, which corresponds to literature values of 938 $kg_{CO2\text{-}eq}$/MWh [44] and 990 $kg_{CO2\text{-}eq}$/MWh [59]. The validity of the LCA model is confirmed by comparing the GWP of the PP-only scenario to the published results. However, the slightly higher value obtained in this study indicates that a conservative LCI has been used, which may lead to some overestimation of the GWP.

It is clear that the SP-PCC unit produces the lowest amount of CO_2 per MWh power output. This is because SP-PCC does not impose any energy penalty on the PP steam cycle, allowing for electrical energy output at full capacity relative to CO_2 emissions. While SP-PCC causes slightly higher emissions to be released compared to the conventional PCC and SA-PCC (23 % SF) at the same CO_2 capture rate, it compensates for this by eliminating the energy penalty. This results in the PP emitting less CO_2 at a constant power output, lowering the overall GWP/MWh and related environmental burdens. There is, however, only a slight difference between the measured 903 $kg_{CO2\text{-}eq}$/MWh for SA-PCC (100 % SF) and 865 $kg_{CO2\text{-}eq}$/MWh for SP-PCC, which motivates a sensitivity analysis to be undertaken. Fig. 8 also shows a breakdown of the key emission categories that make up the GWP to better understand the differences between the five scenarios. This also helps in identifying the hotspots for the main emission sources. Obviously, the PP itself produces the majority of the CO_2 emission in all five scenarios. The coal mining and preparation category shows consistent GWP impact across all five scenarios since the coal intake would be almost equivalent. The electricity demand and the emissions related to the PCC operation also show consistent GWP impact. However, two new emission categories visibly emerge in the SA-PCC (100 % SF) and SP-PCC scenarios related to the massive HTF (for thermal energy storage) and MEA (for solvent storage) usage in these two scenarios, respectively. Despite this, the emissions per energy unit (MWh) convey the advantages of the SP-PCC process compared to other scenarios. This is because SP-PCC does not contribute an energy penalty to the power-plant, meaning that more electrical output is generated by the power-plant relative to the CO_2 emissions. Thus, even though the SP-PCC unit causes greater emissions per mass unit (3,234 $kg_{CO2\text{-}eq}$) than conventional PCC (3,129 $kg_{CO2\text{-}eq}$) and SA-PCC (3,123 $kg_{CO2\text{-}eq}$) at the same CO_2 capture rate, the SP-PCC makes up for this by removing the energy penalty and causing the overall power-plant to emit less CO_2 for constant energy output. The emissions abatement measure, on the other hand, accounts for curbing emissions to reduce the concentration of GHG in the atmosphere. Fig. 9 illustrates the reduction in CO_2 emissions achieved through carbon capture scenarios relative to the baseline. The baseline considered here is the PP-only scenario, and the reduction in GHG emissions for each capture scenario is determined by subtracting the corresponding GWP from the baseline. Higher values indicate a greater curb in GHG emissions. The results show that the intrusion of solar energy at a 23 % SF only slightly improves the GWP abatement (Fig. 9-a). This is because the addition of solar components leads to an increase in CO_2 emissions from solar material production, installation, and change of land use, which offsets the decrease in CO_2 emissions from electricity generation. As a result, the

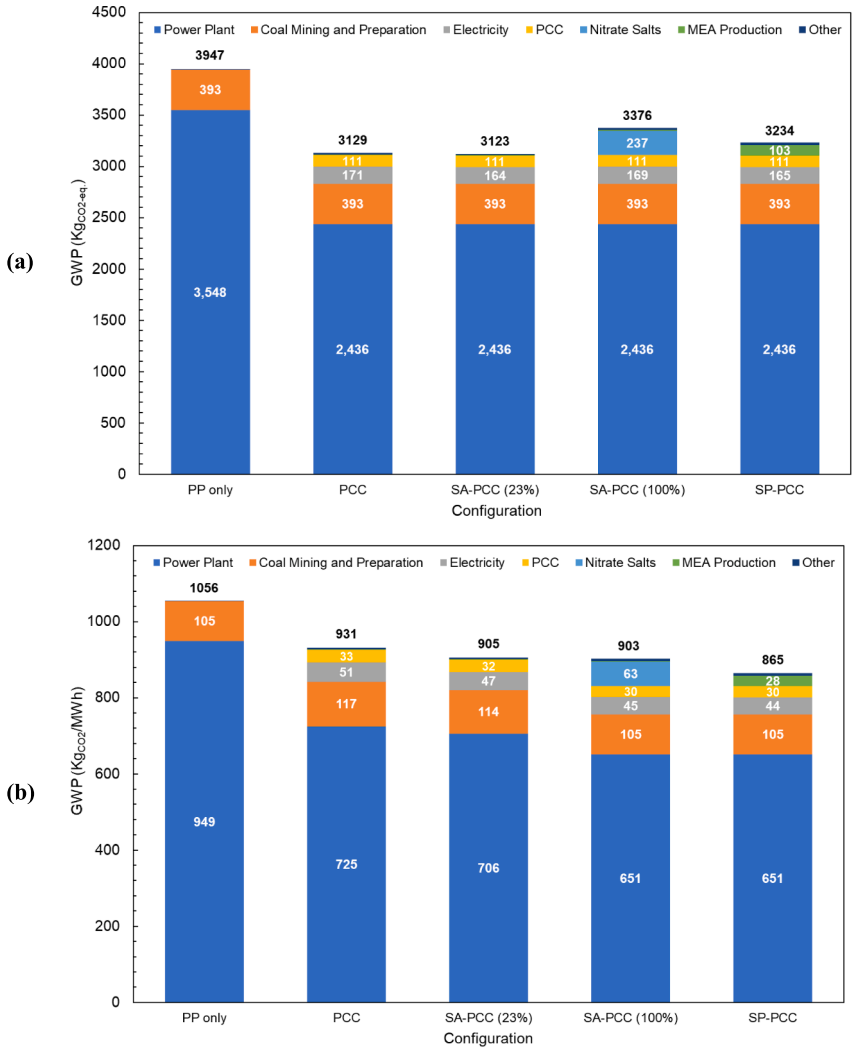

Fig. 8. Global warming potential in reference to 660MW$_e$ PP stacked by the source of emissions: (a) the net GWP (Kg$_{CO2-eq}$) as calculated by OpenLCA; (b) the GWP levelized by the PP electrical output (Kg$_{CO2}$/MWh). 'Power plant' refers to emissions caused by the PP, and 'Electricity' refers to the emissions resulted from power consumption in the PCC.

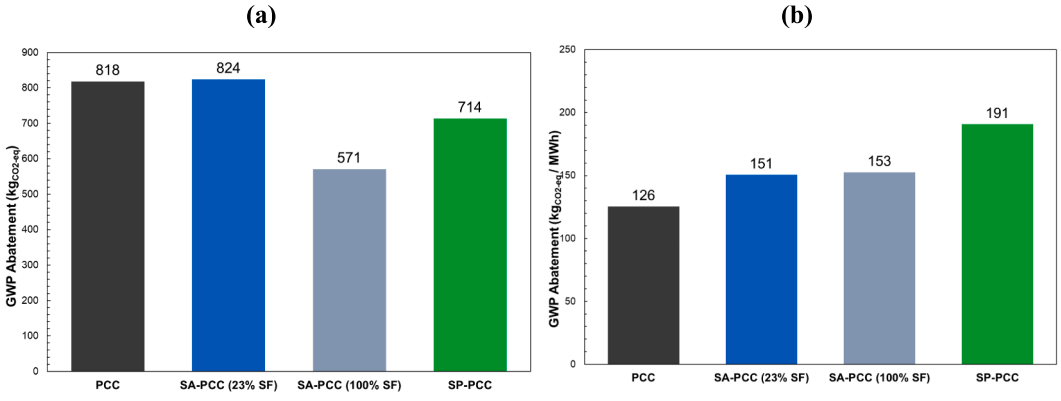

Fig. 9. The GWP abatement for each carbon capture scenario relative to the power-plant only baseline, in terms of kg$_{CO2-eq}$ emitted per tonne CO_2 captured (a) and kg$_{CO2-eq}$ emitted per MWh$_e$ produced from the power-plant (b).

net effect is marginal.

Another important finding is that the abatement significantly decreases as the SF increases from 23 % to 100 % as a result of constructing larger TES and bulkier nitrate-salt HTF. Conversely, the SP-PCC arrangement outperforms the 100 % SA-PCC system by 25 % in terms of GHG emissions abatement. This difference can be attributed to the extensive use of nitrate salts in the 100 % SA-PCC system, which results in a higher GWP. On the contrary, the SP-PCC arrangement employs a larger solar field and a bulk of MEA, leading to a 12.82 % and 13.34 % decrease in abatement compared to the standalone PCC and 23 % SA-

PCC arrangements, respectively. Fig. 9-b confirms that the SP-PCC arrangement achieves the highest GHG emissions abatement per unit of energy output (191 $kg_{CO2\text{-}eq}$/MWh), an improvement of 51.6 % to the conventional PCC and 24.8–26.5 % compared to the SA-PCC scenarios, and thereby would provide a noticeable advantage for the best solar integration approach.

3.2. Sensitivity analysis

It is evident that the effectiveness of all carbon capture scenarios relative to the standalone 660MW_e PP is marginal. Fig. 8-b indicates that capturing the CO_2 in the PCC has reduced the emission intensity of power production by 11.9 %, 14.3 %, 14.5 %, and 18.1 % for the PCC, SA-PCC (23 % SF), SA-PCC (100 % SF), and SP-PCC scenarios, respectively. The reason for such a low emission reduction potential is related to the capture target capped at 1.5 M $tonne_{CO2}$/y which requires the processing of only 34 % of the flue gas at full PP capacity. Certainly, processing more flue gas or comparing that with PPs at lower production capacities would show more significant results. To evaluate the effectiveness of GWP reductions at a higher capture rate of various PCC technologies, a sensitivity analysis is carried out by examining a scenario where the PP capacity was reduced by half, to 330MW_e but at the same capture capacity of 1.5 Mt/y. In this system, the flue gas from the PP that is processed by the PCC unit is increased to 68 %, which is doubled compared to the specified 34 %, while the mass capture rate is kept constant at 1.5 Mt/y. This means that the variables that no longer remain constant are the coal mass requirements, power-plant construction requirements, and power-plant waste disposal and emissions, which are halved due to the lower energy production capacity. For the five scenarios, the environmental impact factors are estimated using the same ReCiPe Midpoint method (Supplementary Materials [54,62,63]) and directly compared with the 660MW_e conditions in Fig. 10. Overall, the spider charts reveal that increasing the flue gas processing rate reduces the environmental burden for all impact categories across the five scenarios. This trend is evident as a consequence of the PP energy capacity being halved to the 330MW_e.

Examining each of the impact categories, there is an increasing trend for the ionising radiation, human toxicity, ozone depletion, marine and freshwater eutrophication across the five scenarios. These criteria are relatively high as a result of the significant amount of MEA solvent being produced and used in the SP-PCC scenario. The ecotoxicity of marine, terrestrial and freshwater conditions also increase when comparing the PP-only design to the conventional PCC and the integration of solar energy via SA-PCC and SP-PCC. On the other hand, the impact factors of climate change, terrestrial acidification, photochemical oxidant formation and particulate matter formation for the SP-PCC system, relative to the other scenarios, proved to be advantageous in reducing the GHG impact. Table 9 shows the data for the impact assessment for all environmental factors illustrated in the spider charts. It provides a side-by-side comparison of the two different PP capacities investigated: the 330MW_e and 660MW_e, respectively. Therefore, it indicates that trade-offs need to be made when assessing the environmental viability of commercial applications, to ultimately reduce the emissions produced in each scenario.

Focusing on the mitigation of climate change via the GWP index, Fig. 11 compares this impact category across all five scenarios at the two different PP capacities: 330MW_e and 660MW_e. It is evident in Fig. 11-a that a lower PP energy output has resulted in lower GWP values for all PCC systems relative to the PP-only scenario, in comparison to the 660MW_e condition. The GWP computed for 330MW_e PP became less than half of the 660MW_e GWP, despite the flue gas flowrate being doubled. The reason for this is because the PP is releasing fewer emissions into the atmosphere, since the flue gas processing rate in the PCC scenarios has risen. Examining Fig. 11-b, the PP-only scenario maintains a relatively consistent value between the two PP capacities. The GWP is calculated based on CO_2 emissions, which are proportional to the electrical energy generated by the PP. However, the GWP per energy unit (MWh) for the 330MW_e capacity has been lowered, in the PCC scenarios, as a larger portion of emissions is being treated and processed.

The percentage abatement of GWP relative to the PP-only scenario, for both 660MW_e and 330MW_e capacities is presented in Fig. 12. The SP-PCC has the highest percentage abatement of GHG emissions and is

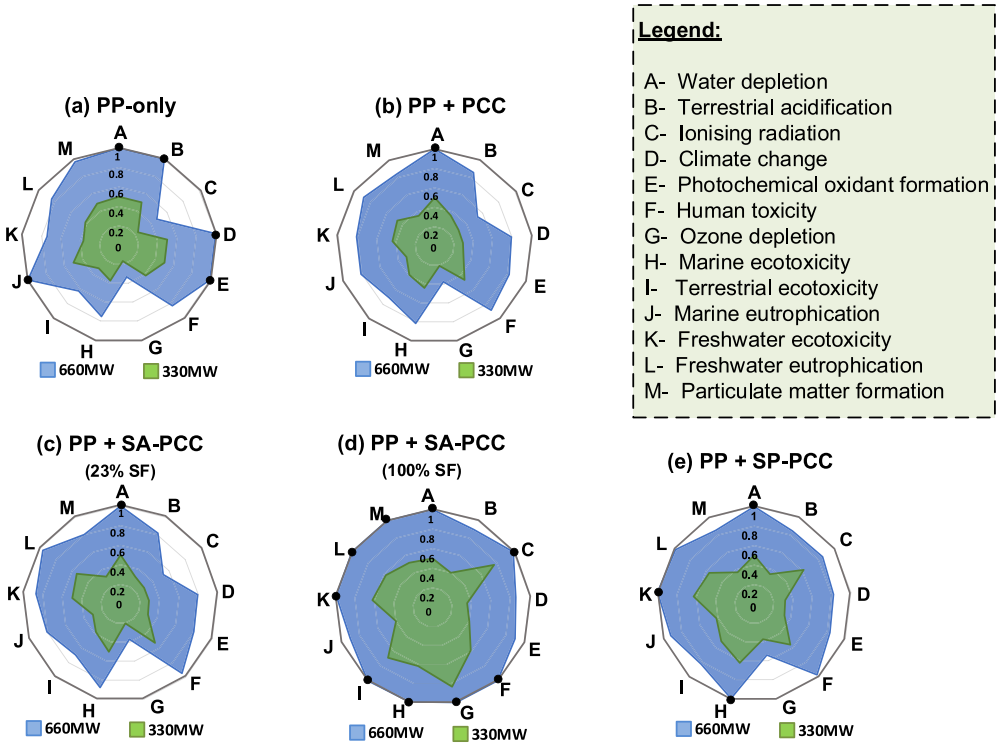

Fig. 10. Spider charts illustrating thirteen impact categories for 660 MW and 330 MW PPs across five scenarios.

Table 9
Summary of impact results for 660 MW and 330 MW from ReCiPe midpoint impact assessment method.

Name	PP-only		PP + PCC		PP + SA-PCC (23 % SF)		PP + SA-PCC (100 % SF)		PP + SP-PCC	
Capacity (MW_e)	330	660	330	660	330	660	330	660	330	660
Water depletion (m^3)	3.92×10^{-3}	7.84×10^{-3}	3.92×10^{-3}	7.84×10^{-3}	3.92×10^{-3}	7.84×10^{-3}	3.92×10^{-3}	7.84×10^{-3}	3.92×10^{-3}	7.84×10^{-3}
Terrestrial acidification ($kg_{SO2\text{-}eq}$)	7.22	14.44	5.15	12.37	4.58	11.80	5.77	12.99	5.00	12.22
Ionising radiation ($kg_{U235\text{-}eq}$)	3.54	7.06	4.44	7.97	4.36	7.89	11.42	14.95	9.22	12.75
Climate change ($kg_{CO2\text{-}eq}$)	1972.88	3947.04	1155.70	3128.57	1149.92	3122.80	1403.11	3375.99	1260.61	3233.49
Photochemical oxidant formation (kg_{NMVOC})	5.05	10.11	3.21	8.27	3.02	8.08	4.05	9.10	3.35	8.41
Human toxicity ($kg_{1,4\text{-}DCB\text{-}eq}$)	518.33	1036.57	578.37	1096.66	663.68	1181.97	733.26	1251.55	699.30	1217.58
Ozone depletion ($kg_{CFC\text{-}11\text{-}eq}$)	4.98×10^{-6}	9.99×10^{-6}	6.24×10^{-6}	1.12×10^{-5}	6.11×10^{-6}	1.11×10^{-5}	2.51×10^{-5}	3.01×10^{-5}	1.12×10^{-5}	1.62×10^{-5}
Marine ecotoxicity ($kg_{1,4\text{-}DCB\text{-}eq}$)	12.66	25.55	14.96	27.74	17.03	29.80	20.96	33.74	21.21	33.99
Terrestrial ecotoxicity ($kg_{1,4\text{-}DCB\text{-}eq}$)	2.31×10^{-2}	4.61×10^{-2}	2.90×10^{-2}	5.20×10^{-2}	2.80×10^{-2}	5.11×10^{-2}	5.06×10^{-2}	7.37×10^{-2}	3.76×10^{-2}	6.07×10^{-2}
Marine eutrophication ($kg_{N\text{-}eq}$)	1.74	3.48	1.08	2.82	1.06	2.80	1.39	3.13	1.45	3.19
Freshwater ecotoxicity ($kg_{1,4\text{-}DCB\text{-}eq}$)	13.28	26.83	15.77	29.19	17.94	31.36	22.36	35.77	22.67	36.08
Freshwater eutrophication ($kg_{P\text{-}eq}$)	0.79	1.59	0.88	1.68	1.03	1.82	1.10	1.89	1.06	1.86
Particulate matter formation ($kg_{PM10\text{-}eq}$)	1.99	3.98	1.45	3.44	1.29	3.28	2.11	4.10	1.51	3.50

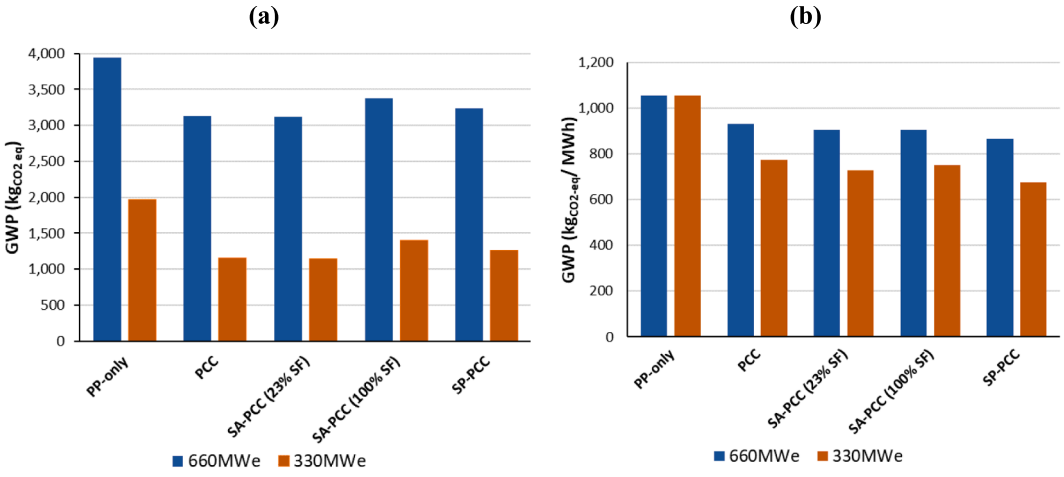

Fig. 11. The GWP Comparison for $660MW_e$ and $330MW_e$ PP capacities: (a) the net GWP for each scenario where all PCC units capture 1 tonne CO_2 and the PP-only scenario operates at the same coal intake to PCC scenarios; (b) the GWP levelized per MWh PP electrical output.

significantly better than other PCC configurations. This analysis supports the fact that SP-PCC is advantageous in minimising the environmental burden of coal-fired PP processes. Additionally, a direct comparison between the $330MW_e$ and $660MW_e$ cases are shown in Fig. 12 indicates that the percentage of GWP abatement for the $330MW_e$ capacity is almost two times higher. This demonstrates that if efforts are made to enhance the capacity of SP-PCC capture, it will result in proportional reductions in the impact of PPs on the environment.

Evidently, the sensitivity analysis reveals that reduced GWP can be improved by having a greater percentage of capture rate. Since the primary objective of CCS technologies is to decrease the GWP/MWh of PPs, the findings prove that SP-PCC is more environmentally advantageous than comparable PCC applications. As a result, another sensitivity analysis is undertaken to determine the optimal conditions for SP-PCC with the lowest overall environmental consequences.

In analysing the GWP abatement in the SP-PCC scenario, the key emission sources would come from two major technology components (SCF vs the solvent storage volume) that may act paradoxically, because increasing the size of the solar field would diminish the need for bulk MEA and large solvent storage. To understand the trade-off between the SCF size and the solvent storage volume, the solar multiple (SM) [60] has been sensitized by 50 % increments to understand the magnitude of these impacts. Hence, if the SCF can regenerate more solvent per time unit, the required solvent amount and storage volume would be decreased resulting in lower environmental impact. Therefore, an LCA is conducted to estimate the GWP for the SP-PCC design by increasing the SM to 1.5, 2.0 and 2.5 for the $660MW_e$ PP capacity. The results are illustrated in Fig. 13, whereby higher SM values will result in a larger SCF size, meaning it can yield more thermal energy and the instant regeneration of the rich solvent. This, in turn, leads to a smaller solvent storage system as the So-St network works more efficiently during the day to desorb the CO_2 from the rich solvent. These factors clearly have an opposing effect on the GWP, which influences the optimized conditions for SP-PCC with the least environmental impact. The decline in the GWP of the solvent storage is however more significant, as it happens at a steeper gradient, compared to the incline in the GWP of the SCF. This is mostly originated from the decrease in MEA solvent demand that would have a substantial contribution to the GWP relative to the materials used in the SCF. Ultimately, this imbalance results in a lower GWP impact for higher SM values. However, giving the cost of SCF installation, engineering, and operation largely driven by the upfront capital costs, the levelized cost of electricity (LCOE) would be proportionally increased

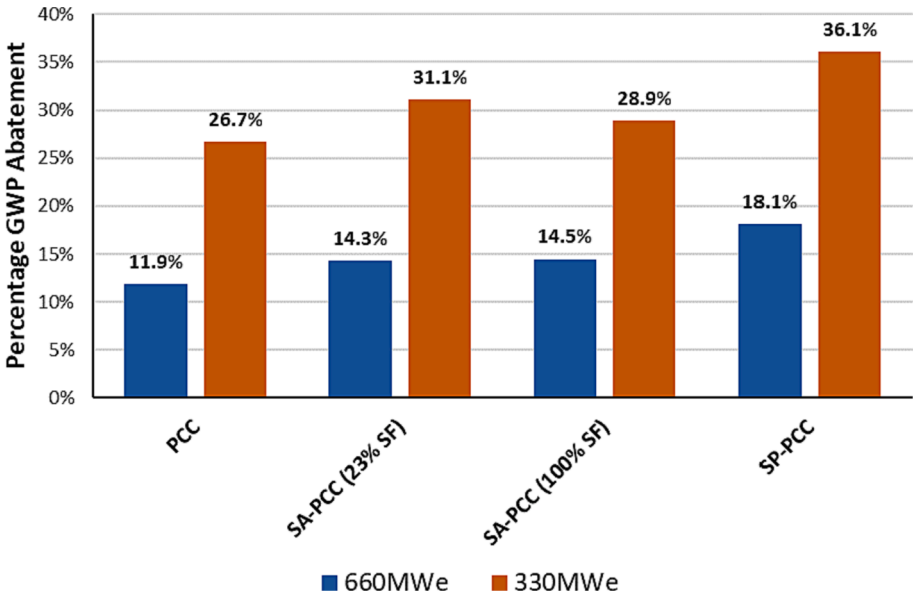

Fig. 12. Comparison of GWP abatement percentage for 660MW$_e$ and 330MW$_e$ PP capacities.

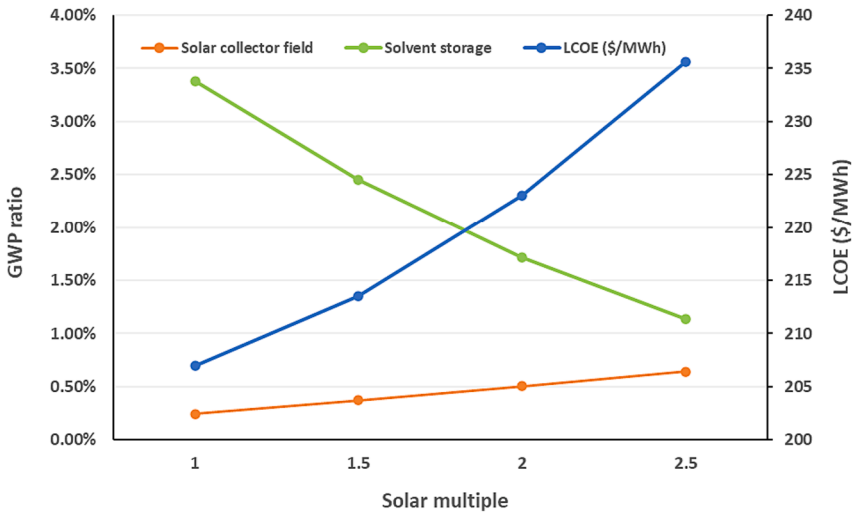

Fig. 13. The GWP for each SM case levelized to the base-case for both SCF (orange line) and solvent storage (green line) impacts and the potential effect on the techno-economics and the levelized cost of electricity (LCOE) as modelled in the previous technoeconomic work [61]. (For interpretation of the references to colour in this figure legend, the reader is referred to the web version of this article.)

from the base case of AU$ 207 when SM = 1 [15] to AU$ 237 when the SM is multiplied by 2.5 folds (SM = 2.5).

In short, this sensitivity analysis confirms that higher SM values, which involve increasing the SCF size and reduced solvent requirements, will lower the GWP impact. The benefits of increasing the SM for the SP-PCC design, however, will incur a proportional cost penalty in the capital and operational expenditure, which must be considered. This study proves that SP-PCC is a promising approach for commercial applications, particularly when sourcing alternative renewable or waste-heat energy sources is a challenge. Therefore, a balance between the environmental impact and the techno-economics must be established for the optimal design and operation of the SP-PCC system.

4. Conclusions

This study performed an LCA to investigate the environmental burdens of the novel SP-PCC process relative to other carbon capture technologies. The LCA results were compared with four other scenarios, including the baseline PP-only, PP with conventional PCC, optimised SA-PCC at 23 % SF and idealised SA-PCC at 100 % SF. Comparing all environmental impact factors, it was found that the integration of solar thermal energy via the SA-PCC and SP-PCC configurations modestly decreased GWP for a 660MW$_e$ PP. Carbon capture technologies, however, did not provide major improvements in other environmental categories such as ionising radiation, human toxicity, ozone depletion, marine and freshwater eutrophication.

The findings revealed that the SP-PCC design emits the lowest amount of CO_2 per MWh output of the PP, with a GWP measured at 865 kg$_{CO2\text{-}eq}$/MWh. This is directly compared with another PP at the half capacity of 330MW$_e$, which showed that an increase in the capture rate percentage resulted in a greater reduction of the GWP since a higher portion of the flue gas was processed and more CO_2 was captured. The effect of SP-PCC technology was more visible in GHG emissions abatement potential where it showed an improvement of 51.6 % compared to the conventional PCC and ~25–26 % to compared to the SA-PCC scenarios. The reason for such a low emission reduction potential was

attributed to the capture target capped at 1.5 M tonne$_{CO2}$/y which requires the processing of only 34 % of the flue gas at full PP capacity. Nonetheless, when the PP capacity was reduced by half to 330MW$_e$ at the same capture rate of 1.5 Mt/y, the results showed significant improvements in all impact categories. More insight on the key SP-PCC components revealed that sizing/designing the SCF and solvent amount/storage would act paradoxically in terms of GHG emissions potential, as higher SM values have increased the GWP abatement, because larger SCF size would lower the need for more MEA solvent and reduce the storage volume requirements. Although, an increase in SM did not make the process more economically viable because there was an increased burden for the CAPEX and OPEX. In essence, SP-PCC was highly beneficial to preserve steam for power production, and it was independent from the operation and control of the PP, eliminating the energy penalty and preserving the steam for power production only. This resulted in an overall reduction of the GWP per unit of energy produced by the PP. However, the analysis of environmental consequences must extend beyond GHG emissions, and this study demonstrated that trade-offs between life cycle and techno-economics need to be optimized.

Declaration of Competing Interest

The authors declare that they have no known competing financial interests or personal relationships that could have appeared to influence the work reported in this paper.

Data availability

Data will be made available on request.

Acknowledgment

The authors would like to thank the Department of Regional New South Wales for their financial support provided through the Coal Innovation New South Wales Fund (RDE493-30).

Appendix A. Supplementary material

Supplementary data to this article can be found online at https://doi.org/10.1016/j.enconman.2023.117745.

References

[1] Jackson R, et al. Global fossil carbon emissions rebound near pre-COVID-19 levels. Environ Res Lett 2022;17(3):031001.
[2] World Coal Association. Coal & electricity; 2021 [cited 1/4 /2023]; Available from: https://www.worldcoal.org/coal-facts/coal-electricity/.
[3] Erans M, et al. Direct air capture: process technology, techno-economic and socio-political challenges. Energ Environ Sci 2022;15(4):1360–405.
[4] Deutz S, Bardow A. Life-cycle assessment of an industrial direct air capture process based on temperature–vacuum swing adsorption. Nat Energy 2021;6(2):203–13.
[5] IPCC. Global warming of 1.5° C: an IPCC special report on the impacts of global warming of 1.5° C above pre-industrial levels and related global greenhouse gas emission pathways, in the context of strengthening the global response to the threat of climate change, sustainable development, and efforts to eradicate poverty: Intergovernmental Panel on Climate Change; 2018.
[6] Abdul Manaf N., et al. Model-based optimisation of highly-integrated renewables with post-combustion carbon capture processes. ANLEC R&D; 2016. URL: https://anlecrd.com.au/projects/model-based-optimisation-of-highly-integrated-post-combustion-carbon-capture-processes/.
[7] Mostafavi E, Ashrafi O, Navarri P. Assessment of process modifications for amine-based post-combustion carbon capture processes. Clean Eng Technol 2021;4:100249.
[8] Qadir A, et al. Potential for solar-assisted post-combustion carbon capture in Australia. Appl Energy 2013;111:175–85.
[9] Mokhtar M, et al. Solar-assisted post-combustion carbon capture feasibility study. Appl Energy 2012;92:668–76.
[10] Parvareh F, et al. Integration of solar energy in coal-fired power plants retrofitted with carbon capture: a review. Renew Sustain Energy Rev 2014;38:1029–44.
[11] Parvareh F, et al. Solar repowering of PCC-retrofitted power plants; solar thermal plant dynamic modelling and control strategies. Sol Energy 2015;119:507–30.
[12] Cau G, Cocco D, Tola V. Performance assessment of USC power plants integrated with CCS and concentrating solar collectors. Energ Conver Manage 2014;88:973–84.
[13] Khalilpour R, et al. A novel process for direct solvent regeneration via solar thermal energy for carbon capture. Renew Energy 2017;104:60–75.
[14] Milani D, et al. Analysis for a solar stripper design for carbon capture under transient conditions. Int J Heat Mass Transf 2021;166:120799.
[15] Milani D, et al. A novel design protocol for solar-powered carbon capture. Therm Sci Eng Prog 2021;26:101059.
[16] Nelson S, et al. A CFD study of a direct solar-driven desorption process for carbon capture under transient conditions. Sustainable Energy Technol Assess 2021;47:101516.
[17] Milani D, et al. Process control strategies for solar-powered carbon capture under transient solar conditions. Energy 2022;239:122382.
[18] Milani D, et al. Solar-powered PCC: an upfront levy for sustainable carbon capture. Int J Greenhouse Gas Control 2022;115:103611.
[19] Terlouw T, et al. Life cycle assessment of direct air carbon capture and storage with low-carbon energy sources. Environ Sci Technol 2021;55(16):11397–411.
[20] da Cruz TT, et al. Life cycle assessment of carbon capture and storage/utilization: from current state to future research directions and opportunities. Int J Greenhouse Gas Control 2021;108:103309.
[21] Klüppel H-J. The revision of ISO standards 14040-3-ISO 14040: environmental management–life cycle assessment–principles and framework-ISO 14044: environmental management–life cycle assessment–requirements and guidelines. Int J Life Cycle Assess 2005;10(3):165.
[22] Goglio P, et al. Advances and challenges of life cycle assessment (LCA) of greenhouse gas removal technologies to fight climate changes. J Clean Prod 2020;244:118896.
[23] Müller LJ, et al. A guideline for life cycle assessment of carbon capture and utilization. Front Energy Res 2020;8:15.
[24] Zhang X, et al. Post-combustion carbon capture technologies: Energetic analysis and life cycle assessment. Int J Greenhouse Gas Control 2014;27:289–98.
[25] Matin NS, Flanagan WP. Life cycle assessment of amine-based versus ammonia-based post combustion CO2 capture in coal-fired power plants. Int J Greenhouse Gas Control 2022;113:103535.
[26] Petrescu L, et al. Life cycle assessment for supercritical pulverized coal power plants with post-combustion carbon capture and storage. J Clean Prod 2017;157:10–21.
[27] Wang J, et al. Application potential of solar-assisted post-combustion carbon capture and storage (CCS) in China: a life cycle approach. J Clean Prod 2017;154:541–52.
[28] Manuilova A, et al. Life cycle assessment of post-combustion CO2 capture and CO2-enhanced oil recovery based on the Boundary Dam Integrated Carbon Capture and Storage Demonstration Project in Saskatchewan. Energy Proc 2014;63:7398–407.
[29] Carpentieri M, Corti A, Lombardi L. Life cycle assessment (LCA) of an integrated biomass gasification combined cycle (IBGCC) with CO2 removal. Energ Conver Manage 2005;46(11–12):1790–808.
[30] Weihs GF, et al. Life cycle assessment of co-firing coal and wood waste for bio-energy with carbon capture and storage–New South Wales study. Energ Conver Manage 2022;273:116406.
[31] Xie S, et al. Coal power decarbonization via biomass co-firing with carbon capture and storage: Tradeoff between exergy loss and GHG reduction. Energ Conver Manage 2023;288:117155.
[32] de Jonge MM, et al. Life cycle carbon efficiency of Direct Air Capture systems with strong hydroxide sorbents. Int J Greenhouse Gas Control 2019;80:25–31.
[33] Manaf NA, Milani D, Abbas A. An intelligent platform for evaluating investment in low-emissions technology for clean power production under ETS policy. J Clean Prod 2021;317:128362.
[34] Li K, et al. Systematic study of aqueous monoethanolamine (MEA)-based CO2 capture process: techno-economic assessment of the MEA process and its improvements. Appl Energy 2016;165:648–59.
[35] Tsupari E, et al. Post-combustion capture of CO2 at an integrated steel mill–Part II: economic feasibility. Int J Greenhouse Gas Control 2013;16:278–86.
[36] Dave N, et al. Impact of liquid absorption process development on the costs of post-combustion capture in Australian coal-fired power stations. Chem Eng Res Des 2011;89(9):1625–38.
[37] Wang J, et al. Water-energy-carbon nexus: a life cycle assessment of post-combustion carbon capture technology from power plant level. J Clean Prod 2021;312:127727.
[38] Grant T, Anderson C, Hooper B. Comparative life cycle assessment of potassium carbonate and monoethanolamine solvents for CO2 capture from post combustion flue gases. Int J Greenhouse Gas Control 2014;28:35–44.
[39] Dong Z, et al. Life cycle assessment of coal-fired solar-assisted carbon capture power generation system integrated with organic Rankine cycle. J Clean Prod 2022;356:131888.
[40] Harvey J et al. Pavement life cycle assessment framework. United States: Federal Highway Administration; 2016.
[41] Argoti A, Orjuela A, Narváez PC. Challenges and opportunities in assessing sustainability during chemical process design. Curr Opin Chem Eng 2019;26:96–103.
[42] Krishna IM et al. Environmental management: science and engineering for industry. Butterworth-Heinemann; 2017.
[43] Peralta ME, Alcalá N, Soltero VM. Weighting with life cycle assessment and cradle to cradle: a methodology for global sustainability design. Appl Sci 2021;11(19):9042.

[44] Fimbres Weihs GA, et al. Feasibility assessment of Bioenergy with Carbon Capture and Storage (BECCS) deployment with Municipal Solid Waste (MSW) co-combustion at New South Wales (NSW) coal power plants. Coal Innovation NSW Fund Round 3 seed grants. 2020.
[45] Milani D, et al. Tailored solar field and solvent storage for direct solvent regeneration: a novel approach to solarise carbon capture technology. Appl Therm Eng 2020;171:115119.
[46] Ou Y, Zhai H, Rubin ES. Life cycle water use of coal-and natural-gas-fired power plants with and without carbon capture and storage. Int J Greenhouse Gas Control 2016;44:249–61.
[47] Spath PL, Mann MK, Kerr DR. Life cycle assessment of coal-fired power production. Golden, CO (United States): National Renewable Energy Lab. (NREL); 1999.
[48] Milani D, et al. A model-based analysis of CO2 utilization in methanol synthesis plant. J CO2 Util 2015;10:12–22.
[49] Turton R et al. Analysis, synthesis and design of chemical processes. Pearson Education; 2008.
[50] Klein SJ, Rubin ES. Life cycle assessment of greenhouse gas emissions, water and land use for concentrated solar power plants with different energy backup systems. Energy Policy 2013;63:935–50.
[51] Yujia W, Zhaofeng X, Zheng L. Lifecycle analysis of coal-fired power plants with CCS in China. Energy Proc 2014;63:7444–51.
[52] Koornneef J, et al. Life cycle assessment of a pulverized coal power plant with post-combustion capture, transport and storage of CO2. Int J Greenhouse Gas Control 2008;2(4):448–67.
[53] Knoope M, Ramírez A, Faaij A. Economic optimization of CO2 pipeline configurations. Energy Proc 2013;37:3105–12.
[54] Goedkoop M et al. *ReCiPe 2008*. A life cycle impact assessment method which comprises harmonised category indicators at the midpoint and the endpoint level. 2009;1:1–126.
[55] Fazio SB, Zampori L, Sala S, Diaconu E. Supporting information to the characterisation factors of recommended EF Life Cycle Impact Assessment methods. JRC Publications Repository.
[56] Jang H-J, Ahn Y-H, Tae S-H. Proposal of major environmental impact categories of construction materials based on life cycle impact assessments. Materials 2022;15 (14):5047.
[57] Koiwanit J, et al. A life cycle assessment study of a Canadian post-combustion carbon dioxide capture process system. Int J Life Cycle Assess 2014;19:357–69.
[58] Chau CK, Leung T, Ng W. A review on life cycle assessment, life cycle energy assessment and life cycle carbon emissions assessment on buildings. Appl Energy 2015;143:395–413.
[59] Odeh NA, Cockerill TT. Life cycle GHG assessment of fossil fuel power plants with carbon capture and storage. Energy Policy 2008;36(1):367–80.
[60] Montes M, et al. Solar multiple optimization for a solar-only thermal power plant, using oil as heat transfer fluid in the parabolic trough collectors. Sol Energy 2009; 83(12):2165–76.
[61] Milani D, et al. Techno-economic analysis of 'Solar-Powered' post-combustion carbon capture. Proceedings of the 15th greenhouse gas control technologies conference. 2021.
[62] Huijbregts MA, et al. ReCiPe2016: a harmonised life cycle impact assessment method at midpoint and endpoint level. Int J Life Cycle Assess 2017;22:138–47.
[63] Huijbregts M et al. ReCiPe2016_CFs_v1.1_20180117, R.v.V.e. Milieu. Ministerie van Volksgezondheid, Welzijn en Sport; 2018.